Aerosol and Air Quality Research, 18: 938–956, 2018

ISSN: 1680-8584 print / 2071-1409 online
doi: 10.4209/aaqr.2017.05.0181

Chemical Characteristics and Source Apportionment of $PM_{2.5}$ and Long-range Transport from Northeast Asia Continent to Niigata in Eastern Japan

Ping Li[1,2*], Keiichi Sato[3], Hideo Hasegawa[4], Minqun Huo[3], Hiroaki Minoura[3], Yayoi Inomata[3], Naoko Take[3], Akie Yuba[3], Mari Futami[3], Tsukasa Takahashi[3], Yuka Kotake[3]

[1] *Graduate School of Science and Technology, Niigata University, Niigata 950-2181, Japan*
[2] *College of Chemistry and Chemical Engineering, Qiqihaer University, Qiqihar 161000, China*
[3] *Asia Center for Air Pollution Research, Niigata-shi 950-2144, Japan*
[4] *Institute of Science and Technology, Niigata University, Niigata 950-2181 Japan*

ABSTRACT

Seasonal intensive sampling was undertaken for two weeks during each of four seasons from May 2015 to February 2017 at Niigata-Maki station in Niigata, eastern Japan. Daily mean concentrations of $PM_{2.5}$ ranged from 4.2 μg m^{-3} to 33.4 μg m^{-3} during the observation period, which were lower than Japanese Environmental Quality Standard for $PM_{2.5}$ (35 μg m^{-3}). The higher concentrations of SO_4^{2-}, NH_4^+ and OC were observed in spring and summer, which may result from photochemical activity and secondary OC production. The major chemical components of $PM_{2.5}$ at Niigata-Maki site were SO_4^{2-}, NO_3^-, NH_4^+, OCM, EC and crustal elements. Compared with data at other urban sites, a lower concentration of EC and NO_3^- and higher OC/EC ratio were observed at Niigata-Maki site, which may result from no significant stationary source and low vehicular traffic in the rural site. $PM_{2.5}$ source apportionment was characterized by positive matrix factorization (PMF) analysis, and the results inferred four major sources: sea salt (10.2%), biomass combustion (18.9%), soil dust (13.2%) and secondary aerosol (44.4%). The potential source contribution function (PSCF) analysis suggested that the major sources of secondary aerosol and sea salts were domestic in southwest Japan and the Sea of Japan, whereas the sources of biomass combustion and soil dust in specific seasons were long range transportation from the Northeast Asian continent (NEA). Comparing with previous studies in western Japan, this study showed a large domestic contribution of southwest Japan for secondary aerosol, while a larger contribution of the NEA was observed in the previous studies. Significant contribution of biomass combustion from northeast China in autumn, and local area in Niigata and southwest Japan in the other seasons was uniquely observed in this study.

Keywords: Secondary aerosol; Biomass combustion; Northeast Asian continent; PMF; PSCF.

INTRODUCTION

Fine particulate matter ($PM_{2.5}$) is considered as an important environmental pollutant and has adverse effects on human health, including effects on the heart, nervous, and vascular system (Zeller *et al*., 2006; Chan *et al*., 2006; Leiva G *et al*., 2013). It is also well documented in various investigations that particulate matter has influence on human health in Japan (Murakami *et al*., 2006; Yamazaki *et al*., 2007). Moreover, $PM_{2.5}$ is proved to be linked to degradation of visual range, with the features of light extinction (Yang *et al*., 2007). To evaluate these effects, components of $PM_{2.5}$ need to be investigated at different temporal and spatial scales because chemical properties in $PM_{2.5}$ are important factors to determine the effects.

Previous studies have investigated chemical components and their variations of $PM_{2.5}$ in Japan, and the long range transport from East Asia countries. For example, secondary and carbonaceous aerosols are associated mostly with $PM_{2.5}$ while Cl^-, Na^+, Ca^{2+} and Mg^{2+} are dominant in the coarse particulate matter of $PM_{2.5\text{-}10}$ and $PM_{>10}$ in Yokohama, a megacity in Tokyo metropolitan area (Khan *et al*., 2010). SO_4^{2-}, NO_3^-, NH_4^+, OC and EC are the major chemical components in Chiba Prefecture, located in Tokyo metropolitan area of Japan, and seasonal fluctuations of EC and OC show that autumn and winter concentrations are relatively higher than those recorded in spring and summer time. This result could be attributed to the impact of burning biomass (Ichikawa *et al*., 2015). The ratios of Cd/Pb and Pb/Zn in $PM_{2.5}$ in the northern Kyushu area of Japan were close to the aerosol composition in Beijing, which implies the same components of $PM_{2.5}$ were transported from the

*Corresponding author.
Tel.: +86-18304525430
E-mail address: liping800214@126.com

NEA to western Japan (Kaneyasu *et al*., 2014). High levels of polycyclic aromatic hydrocarbons (PAHs) in total suspended particles (TSP) are transported from the NEA to western Japan (Coulibaly *et al*., 2015). In addition to observation studies, sensitivity analysis by using a regional chemical transport model demonstrated that contribution from central north China accounts for 50–60% of $PM_{2.5}$ at a remote island in western Japan except in summer (Ikeda *et al*., 2014).

Niigata City is the capital and the most populous city of Niigata Prefecture located in eastern Japan. It lies on the coast of the Sea of Japan and faces the Northeast Asian continent, and the climate is strongly affected by the circulation of the East Asian Monsoon over East Asia, covering eastern China, the Korean Peninsula and Japan. In winter it's dominated by cold currents from the northwest, while in summer the wet and humid currents of tropical origin prevail. Some studies reported that the effects of long-range transport on the areas located downstream of large emission sources play a major role in ambient air quality (Shimadera *et al*., 2009). Since the NEA is upwind with respect to Niigata during the winter monsoon period, $PM_{2.5}$ in Niigata is probably influenced by long-range transport from the NEA. However, few observation studies have focused on fine particles across the coast of the Sea of Japan from the NEA, such as transboundary transport of anthropogenic sulfur in $PM_{2.5}$ (Inomata *et al*., 2016), long-range transport from the NEA of biomass combustion (Huo *et al*., 2016), and long term variations of PAHs in total suspended particles at a background site on Noto Peninsula (Tang *et al*., 2015). Therefore, it is important to identify the sources of $PM_{2.5}$ in a coastal city of the Sea of Japan, such as Niigata, and contribution to long-range transportation from the NEA in order to provide scientific findings for evaluation of atmospheric impact of $PM_{2.5}$ in eastern Japan.

In this research, a field observation study including seasonal intensive measurement of $PM_{2.5}$ was conducted from May 2015 to February 2017 at the Niigata-Maki national acid deposition monitoring station in Niigata, eastern Japan. A comprehensive analysis of thirty three chemical components (including EC, OC, Cl^-, NO_3^-, SO_4^{2-}, Na^+, NH_4^+, K^+, Mg^{2+}, Ca^{2+} and 23 metallic elements) in $PM_{2.5}$ was implemented and the seasonal variations of chemical characteristics in $PM_{2.5}$ were elucidated. Then, statistical analyses of correlation matrix, positive matrix factorization (PMF) for annual and potential source contribution function (PSCF) for annual and specific season were conducted in order to identify major sources of $PM_{2.5}$ in Niigata, and also identify the long-range transport from the NEA.

MATERIAL AND METHODOLOGY

The Monitoring Station

Niigata-Maki national acid deposition monitoring station (37°48’32”, 138°52’10”, 52 m altitude) is located at the foot of Mt. Kakuda (482 m a.s.l.), 1 km from the seashore, and 25 km southwest of the center of Niigata City, the capital of Niigata Prefecture, Japan, as shown in Fig. 1. This station was constructed by the Ministry of the Environment, Japan to monitor acid deposition and air pollutant concentration and to investigate acid deposition in rural areas on the coast of the Sea of Japan. There are no industrial sources near Niigata-Maki site, but a small community (approximately 1300 population) is located 2 km northwest of the station, and thus it is classified as a rural station. Air masses reaching the station are dependent on seasonal wind patterns, which are affected by the monsoon circulation: in winter the northwest cold currents prevail, while in summer they are replaced by the hot and humid currents of the Pacific Ocean.

For the reference data, we used $PM_{2.5}$ data at the Sado-seki national acid deposition monitoring station (38°15’02”, 138°24’01”), which is classified as a remote station, and the Kameda air quality monitoring station (37°52’22”, 139°06’05”), which is classified as an urban station. The

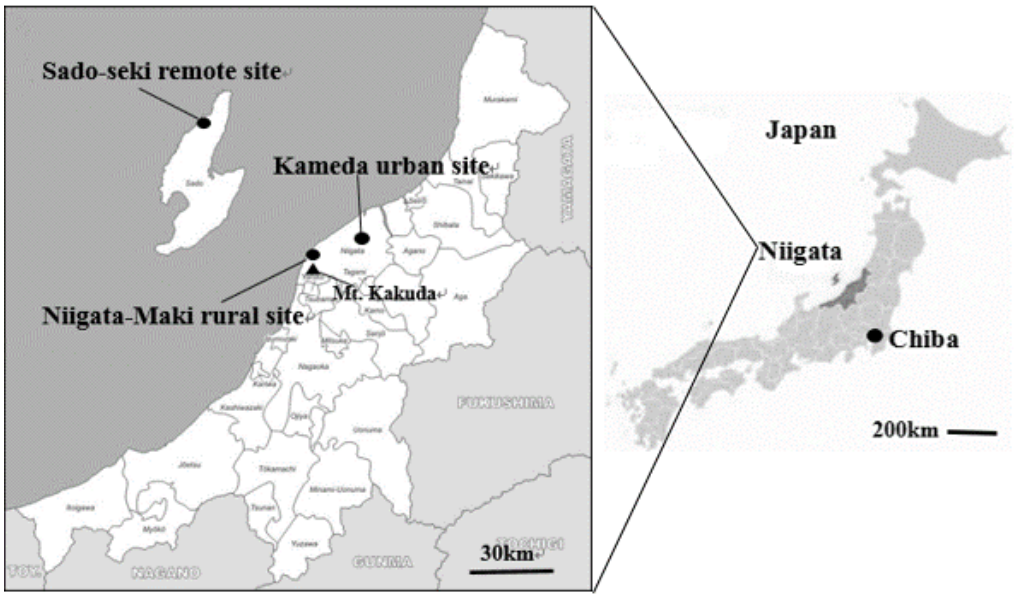

Fig. 1. Location of the study monitoring station: Niigata-Maki and the reference sites: Sado-seki, Kameda, and Chiba.

data of Kameda and Sado-seki sites are cited from the web site of the Ministry of the Environment, Japan (MOEJ) (MOEJ, 2016). Furthermore, we also used the $PM_{2.5}$ continuous monitoring data at the Chiba site located in Tokyo Metropolitan Region of eastern Japan and classified as an urban station. It was conducted as a full year continuous monitoring of $PM_{2.5}$ by a research project (Ichikawa *et al*., 2015). Niigata and Tokyo metropolitan areas are located in eastern Japan. Niigata lies on the Sea of Japan side, whereas Tokyo metropolitan area lies on the Pacific Ocean side. The central mountains of Honshu (Main Island of Japan) are located between them. Therefore, the meteorological conditions and emission sources of both areas would be different, and it is scientifically meaningful to compare the characteristics between them. Moreover, a comprehensive analysis of chemical components in $PM_{2.5}$ was also implemented at the Chiba site, which is comparable to our observational results. Thus, we referred the data at Chiba site on behalf of Tokyo metropolitan area.

Sampling and Chemical Analysis

Daily $PM_{2.5}$ samples were taken for two weeks during each of four seasons from May 2015 to February 2017, and each daily sampling time was conducted from noon to noon of the next day. The sampling periods in this study were the same as the national intensive survey of $PM_{2.5}$ conducted by MOEJ as shown in Table 1. JFY denotes the Japanese fiscal year, which is the period from April to March. We collected a total of 106 daily samples during two years. $PM_{2.5}$ samples were collected on the PTFE membrane filters (Zefluor, 47 mm in diameter and 2.0 μm in pore size, Pall Co., USA) using a sequential FRM sampler (Model 2025, Thermo Fisher Scientific, Inc., USA), designed with a flow rate of 16.7 L min^{-1} and sequential 24-hour sampling for 14 days. The PTFE filters were used for mass concentration, water-soluble ions and metallic elements measurement. $PM_{2.5}$ samples were also collected on the quartz filters (2500QAT-UP, 8 × 10 inches, Pall Co., USA) by using a high volume sampler (HV-1000F, Sibata Scientific Technology Ltd., Japan) and $PM_{2.5}$ impactor (HVI-2.5, Tokyo Dylec Co., Japan), designed with a flow rate of 576 L min^{-1}. By using this high-volume sampler, daily $PM_{2.5}$ sampling was conducted for 7 days (core time). Before and after the core time, 4 days and 3 days continuous sampling were also conducted respectively, so the total sampling period using the high-volume sampler is the same as the sequential FRM sampler (14 days). We used the average concentration for daily data in continuous sampling period. The quartz filters were used for carbonaceous species measurement. The two samplers were set at 5 meters above the ground and 1.5 m above the rooftop. At the Sado-seki site, $PM_{2.5}$ was monitored by continuous β-ray absorption monitor (PM-712, Kimoto Electoric Co., Ltd., Japan). At Kameda and Chiba sites, the same type of FRM sampler as the Niigata-Maki site was used (2025i Sequential Air Sampler Thermo-Scientific Inc., USA, Flow rate: 16.7 L min^{-1} and 24 m^3 day^{-1}).

The mass concentrations of sample filters were determined gravimetrically by using the electronic microbalance (MSE2.7S-000, sensitivity = 0.1 μg, Sartorius AG, Germany) under controlled temperature (20–23°C) and relative humidity (RH at 35–45%). Teflon filters were stored under controlled conditions of temperature and relative humidity for at least 24 hours before and after sampling, and then passed through a static electricity remover before being weighed at least twice. The maximum acceptable difference between the two readings was 3 μg, and all processes were performed in a weighing chamber (PWS-PM2.5, Dylec Co., Japan).

For analyses of water-soluble ion, half of a filter was extracted with 20 mL of Milli-Q water (18.2 MΩ · cm) for 30 minutes by using a shaker (SR-2w, Taitec Co., Japan). The extracted solution was filtered through a pre-washed membrane filter (A045A025A, 25 mm in diameter and 0.45 μm pore size, Advantec Toyo Co., Japan), and stored in a refrigerator at 4°C until chemical analysis. Three anions (Cl^-, NO_3^- and SO_4^{2-}) and five cations (Na^+, NH_4^+, K^+, Mg^{2+} and Ca^{2+}) were determined by ion chromatography (ICS-2100 and ICS-1100, Thermo Fisher Scientific, Inc., USA).

Organic carbon (OC) and elemental carbon (EC) were analyzed by using a Desert Research Institute (DRI, USA) Model 2001A thermal/optical carbon analyzer. Collected quartz filters were punched into 0.505 cm^2 pieces to determine OC and EC by the IMPROVE method with the thermal optical reflection protocol (Chow *et al*., 2001). Depending on combustion temperature and matrix gas, carbonaceous components were fractionated into Organic carbon (OC1–OC4) and Elemental carbon (EC1–EC3), and the optical pyrolysis correction of OC (PyC) by reflectance of helium-neon laser. OC was defined as OC1 + OC2 + OC3 + OC4 + PyC and EC was as EC1 + EC2 + EC3 – PyC.

The concentrations of 23 metallic elements (Al, Fe, Ni, Cr, Zn, Mn, Co, Cu, V, Ga, As, Se, Rb, Sr, Sc, Mo, Cd, Sb, Cs, Ba, Pb, Ag and Hg) were analyzed using an Thermo Fisher XSeries 2 Inductively Coupled Plasma Mass Spectrometry (ICP-MS). A quarter of a PTFE filter was put into a PTFE pressure digestion container, and then dissolved in 6 mL of 70% nitric acid (HNO_3) and 3 mL of 50% hydrofluoric acid (HF) and 1 mL of 30% hydrogen peroxide (H_2O_2). All digestions were performed in a microwave oven (Ethos 900, Milestone General Inc., USA), the steps of the digestion procedure are shown as Table 2. After the microwave digestion procedure, the digestion containers

Table 1. Seasonal intensive sampling periods from May 2015 to February 2017 at Niigata-Maki.

Sampling Year	Spring	Summer	Autumn	Winter
JFY 2015	2015.05.08–2015.05.20	2015.07.22–2015.08.04	2015.10.21–2015.11.03	2016.01.20–2016.02.02
JFY 2016	2016.05.09–2016.05.17	2016.07.21–2016.08.03	2016.10.21–2016.11.03	2017.01.19–2017.02.02

JFY denotes the Japanese fiscal year: JFY 2015 and JFY 2016 is the period from April 2015 to March 2016 and April 2016 to March 2017, respectively.

Table 2. Instrumental parameters for microwave digestion procedure.

step	Time (min.)	Power (w)
1	2	250
2	3	0
3	5	250
4	5	400
5	10	500
6	20	400

were heated until the solution volume is reduced to approximately 0.1 mL so that all of HF is evaporated. Then, the samples were diluted with 1 mol L^{-1} HNO_3 to make a 15 mL solution, was added into both sample and standard solutions. All reagents used for the digestion procedure were ultra-pure grade quality or better, and all regent solutions were prepared using MILLI-Q water. All samples and standards were stored in metal-free centrifuge tubes and kept in a refrigerator at 4°C before analysis.

Quality Assurance (QA) and Quality Control (QC)

The detection limits were calculated as equivalent air concentrations of 3 times of the standard deviations for 8 laboratory blank samples. The detection limits of OC and EC were 0.26 and 0.08 μg m^{-3}, respectively. The detection limits of Na^+, NH_4^+, K^+, Mg^{2+}, Ca^{2+} Cl^-, NO_3^- and SO_4^{2-} were 0.02, 0.01, 0.01, 0.01, 0.01, 0.02, 0.03 and 0.03 μg m^{-3}, respectively. The detection limits of Al, Fe, Ni, Cr, Zn, Mn, Co, Cu, V, Ga, As, Se, Rb, Sr, Sc, Mo, Cd, Sb, Cs, Ba, Pb, Ag and Hg were 22.2, 8.56, 0.03, 1.65, 1.26, 25.7, 1.88, 0.91, 1.83, 14.5, 0.09, 0.36, 0.31, 0.10, 0.53, 0.39, 0.78, 0.13, 0.24, 0.02, 2.02, 0.63 and 0.24 ng m^{-3}, respectively. When the measured concentrations are under these detection limits, we evaluated those as not detected (N.D.).

Working standard samples and ion balance were tested for the water soluble ion analysis by ion chromatography. The original working standard solution of artificial rain water containing 3 anions of Cl^-, NO_3^- and SO_4^{2-} and 5 cations of Na^+, NH_4^+, K^+, Mg^{2+} and Ca^{2+} was obtained by 18th inter-laboratory comparison project on wet deposition in Acid Deposition Monitoring Network in East Asia (EANET) (Network Center for EANET, 2016). Working standard solutions were prepared from the original solution by diluting 100 times with MILLI-Q water. The accuracy of water soluble ion analysis was checked by agreement between the measured values and the prepared values within 15% differences.

We also use ion balance for $PM_{2.5}$ component to check validity of analytical procedure for water soluble ions. The principle of electroneutrality in an extract of $PM_{2.5}$ sample requires that the total anion equivalents equal to the total cation equivalents. According to this principle, ion balance in the extract was checked by the below equation.

$$R = (C - A)/(C + A) \times 100\ (\%) \quad (1)$$

where C and A represents total anion and total cation equivalent concentrations (μeq L^{-1}), and R represents ion balance, respectively. The seasonal variations of water soluble ion balance were shown in Fig. 2, and all seasonal ion balance values were satisfied with the required criteria (Network Center for EANET, 2010).

To check validity of analytical protocol for metallic elements, the Certified Reference Material (CRM) No. 28 Urban Aerosols were used (National Institute for Environmental Studies, 2015). The recoveries of metallic elements were determined by 9 CRM samples, only the recoveries of Sb (75%) less than 80%, and the other metallic elements ranged from 83 to 109%. Therefore, Sb concentration was determined by the recovery ratio, as shown in Table 3. The analytical results were in a good agreement with the certified or reference values within analytical error.

RESULTS AND DISCUSSION

Temporal Variations of $PM_{2.5}$ Mass Concentration

Table 4 shows that the annual mean mass concentrations of $PM_{2.5}$ were 12.3 μg m^{-3} in JFY 2015 and 9.3 μg m^{-3} in JFY 2016, respectively. Although the monitoring was not conducted for a full year, these values were lower than the annual average of the Japanese Environmental Quality Standard (JEQS) for $PM_{2.5}$ (15 μg m^{-3}). Daily mean concentrations of $PM_{2.5}$ ranged from 4.2 μg m^{-3} to 33.4 μg m^{-3} from May 2015 to February 2017, which were lower than the daily average of the JEQS for $PM_{2.5}$ (35 μg m^{-3}), as shown in Fig. 3. Daily $PM_{2.5}$ mass concentrations at Niigata-Maki, Kameda and Sado-seki showed similar temporal trends throughout the observation period. The higher mass concentration days were observed in spring and summer, and the lower mass concentration days were observed in autumn and winter (Fig. 3). The seasonal means are discussed in the following paragraph. Daily $PM_{2.5}$ mass concentrations at Niigata-Maki strongly correlated with those at Kameda ($r = 0.82$, $p < 0.01$) and Sado-seki ($r = 0.80$, $p < 0.01$), which implies these sites are affected by similar sources and local meteorology (Fig. 4).

We compared the seasonal averages of $PM_{2.5}$ mass concentrations with various meteorological parameters of rainfall (mm), wind speed (m s^{-1}), and temperature (°C). The meteorological data was obtained from the nearby monitoring station of the Japan Meteorological Agency (JMA) (JMA, 2017), which is located 6 km southeast of the Niigata-Maki station. As shown in Fig. 5, the seasonal variations of rainfall, wind speed and temperature might effect on the variation of $PM_{2.5}$ concentration. The higher seasonal $PM_{2.5}$ mass concentration is likely to be observed in the higher temperature, windless and less rainfall weather. These meteorological conditions corresponded to higher $PM_{2.5}$ concentrations in spring and summer. Previous studies also showed that higher temperatures often enhance the chemical reactions of atmospheric pollutants (Sanchez-Romero *et al*., 2014; Zhang *et al*., 2015), that strong winds are favorable for the diffusion of air pollutants (Csavina *et al*., 2014), and that $PM_{2.5}$ was negatively correlated to the quantity of accumulated rainfall because of wet removal processes (Ouyang *et al*., 2015).

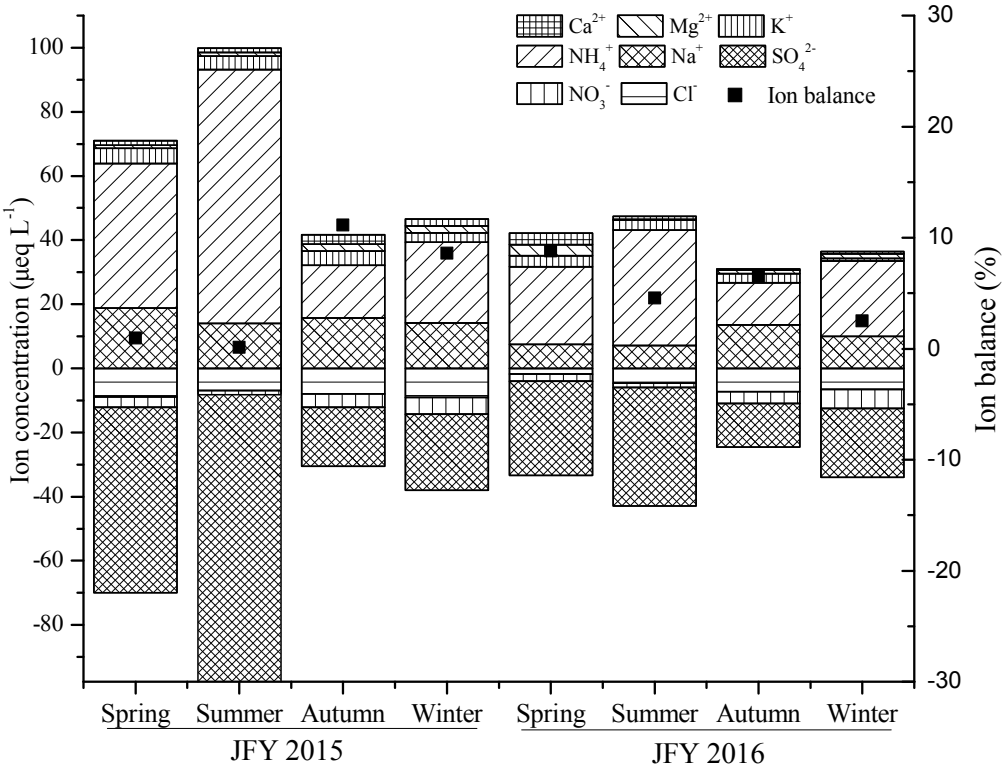

Fig. 2. Seasonal variation of water soluble ion balance.

Table 3. Analytical recoveries of metallic elements in the NIES CRM No.28 Urban Aerosols.

Metallic elements	Unit	Measured Values	Certified or Reference values	Recovery (%)
Al	%	5.13% ± 0.30	5.04% ± 0.10[a]	101.8 ± 6.0
Fe	%	2.77% ± 0.30	2.92% ± 0.17[a]	94.9 ± 10.3
Ni	mg kg^{-1}	66.9 ± 6.0	63.8 ± 3.4[a]	104.9 ± 9.4
Cr	mg kg^{-1}	64.5 ± 6.0	65.6[b]	98.3 ± 9.1
Zn	%	0.12% ± 0.01	0.11% ± 0.010[a]	109.1 ± 9.1
Mn	mg kg^{-1}	678.0 ± 40	686 ± 42[b]	98.8 ± 5.8
Co	mg kg^{-1}	20.7 ± 2.0	22[b]	94.1 ± 9.1
Cu	mg kg^{-1}	112.9 ± 10.0	104 ± 12[a]	108.6 ± 9.6
V	mg kg^{-1}	72.0 ± 6.0	73.2 ± 7.0[a]	98.4 ± 8.2
As	mg kg^{-1}	89.4 ± 6.0	90.2 ± 10.7[a]	99.1 ± 6.7
Se	mg kg^{-1}	14.3 ± 0.7	14.4[b]	99.3 ± 4.9
Rb	mg kg^{-1}	56.7 ± 2.0	64.1[b]	88.5 ± 3.1
Sr	mg kg^{-1}	449.5 ± 14.0	469 ± 16[a]	95.8 ± 3.0
Sc	mg kg^{-1}	10.2 ± 0.6	10.7[b]	95.3 ± 5.6
Mo	mg kg^{-1}	25.8 ± 1.0	28.4[b]	90.8 ± 3.5
Cd	mg kg^{-1}	5.0 ± 0.1	5.6 ± 0.43[a]	89.3 ± 0.9
Sb	mg kg^{-1}	15.0 ± 0.4	20.1[b]	74.6 ± 2.0
Ba	mg kg^{-1}	722.7 ± 16.0	874 ± 65[a]	82.7 ± 1.8
Pb	mg kg^{-1}	357.6 ± 25.0	403 ± 32[a]	88.7 ± 7.1

[a] Certified values, [b] Reference values.

Chemical Characteristics of $PM_{2.5}$

Water Soluble Ions

Since the sampling site is located close to the seashore, it is important to identify the contributions of water soluble ions in $PM_{2.5}$ from non-marine and marine sources. Non-sea-salt ion concentration (nss-*M*) was estimated by the following equation assuming that Na^+ in particulate matter is solely originated from sea salts:

$$C_{\text{nss-}M} = C_M - KC_{Na^+} \quad (2)$$

where *M* is the target ion, *K* is the mass ratio of the target ion to Na^+ in seawater (Mg^{2+} = 0.1190, Ca^{2+} = 0.0382, K^+ = 0.0370, SO_4^{2-} = 0.2515, Cl^- = 1.79) (Kennish *et al*., 1994).

Table 4. Seasonal mean mass concentrations of $PM_{2.5}$, water soluble ionic species, OC and EC at Niigata-Maki.

Season		$PM_{2.5}$	Cl^-	NO_3^-	SO_4^{2-}	Na^+	NH_4^+	K^+
		μg m^{-3}	μg m^{-3}	μg m^{-3}	μg m^{-3}	μg m^{-3}	μg m^{-3}	μg m^{-3}
	Spring	12.9 ± 4.3	0.35 ± 0.32	0.32 ± 0.31	4.61 ± 2.48	0.59 ± 0.41	1.31 ± 0.59	0.24 ± 0.13
JFY	Summer	19.9 ± 9.7	0.32 ± 0.29	0.14 ± 0.12	7.34 ± 5.14	0.47 ± 0.28	2.37 ± 1.69	0.23 ± 0.13
2015	Autumn	9.6 ± 3.1	0.38 ± 0.27	0.43 ± 0.11	1.46 ± 0.76	0.54 ± 0.32	0.47 ± 0.22	0.25 ± 0.09
	Winter	6.8 ± 3.4	0.45 ± 0.19	0.55 ± 0.50	1.88 ± 0.98	0.48 ± 0.18	0.74 ± 0.52	0.16 ± 0.08
Annual mean		12.3 ± 7.5	0.37 ± 0.27	0.36 ± 0.32	3.81 ± 3.73	0.52 ± 0.28	1.22 ± 1.17	0.22 ± 0.11
	Spring	13.2 ± 4.9	0.07 ± 0.19	0.22 ± 0.12	2.34 ± 0.93	0.22 ± 0.19	0.71 ± 0.35	0.19 ± 0.06
JFY	Summer	10.4 ± 3.9	0.18 ± 0.18	0.13 ± 0.11	2.94 ± 1.41	0.21 ± 0.20	1.06 ± 0.50	0.17 ± 0.15
2016	Autumn	6.2 ± 1.8	0.38 ± 0.19	0.37 ± 0.17	1.05 ± 0.27	0.49 ± 0.24	0.36 ± 0.12	0.16 ± 0.07
	Winter	7.3 ± 3.6	0.30 ± 0.29	0.61 ± 0.49	1.70 ± 1.13	0.31 ± 0.25	0.69 ± 0.53	0.03 ± 0.07
Annual mean		9.3 ± 4.2	0.25 ± 0.24	0.34 ± 0.32	2.01 ± 1.08	0.32 ± 0.24	0.70 ± 0.48	0.14 ± 0.11

Season		Mg^{2+}	Ca^{2+}	TWSIs	EC	OC	OC/EC
		μg m^{-3}	μg m^{-3}	μg m^{-3}	μgC m^{-3}	μgC m^{-3}	
	Spring	0.01 ± 0.03	0.01 ± 0.02	7.4	0.74 ± 0.12	2.58 ± 1.01	3.48
JFY	Summer	0.02 ± 0.01	0.03 ± 0.02	10.8	0.86 ± 0.36	2.14 ± 0.76	2.50
2015	Autumn	0.04 ± 0.03	0.08 ± 0.03	3.6	0.61 ± 0.26	1.91 ± 1.02	3.12
	Winter	0.04 ± 0.02	0.05 ± 0.02	4.3	0.44 ± 0.38	0.50 ± 0.28	1.12
Annual mean		0.03 ± 0.02	0.04 ± 0.02	6.5	0.66 ± 0.28	1.78 ± 0.76	2.55
	Spring	0.07 ± 0.01	0.10 ± 0.03	3.9	0.50 ± 0.23	2.34 ± 1.30	4.92
JFY	Summer	N.D.	0.02 ± 0.03	4.7	0.63 ± 0.31	2.09 ± 0.78	3.34
2016	Autumn	0.02 ± 0.01	N.D.	2.9	0.49 ± 0.88	1.20 ± 1.02	2.24
	Winter	0.02 ± 0.02	0.01 ± 0.02	3.6	0.32 ± 0.22	0.79 ± 0.52	2.45
Annual mean		0.03 ± 0.01	0.03 ± 0.02	3.8	0.49 ± 0.41	1.61 ± 0.90	3.24

The values after "±" denote standard deviations based on daily mean concentrations.
TWSIs (Total water-soluble ions) is the summation of Cl^-, NO_3^-, SO_4^{2-}, Na^+, NH_4^+, K^+, Mg^{2+} and Ca^{2+}.

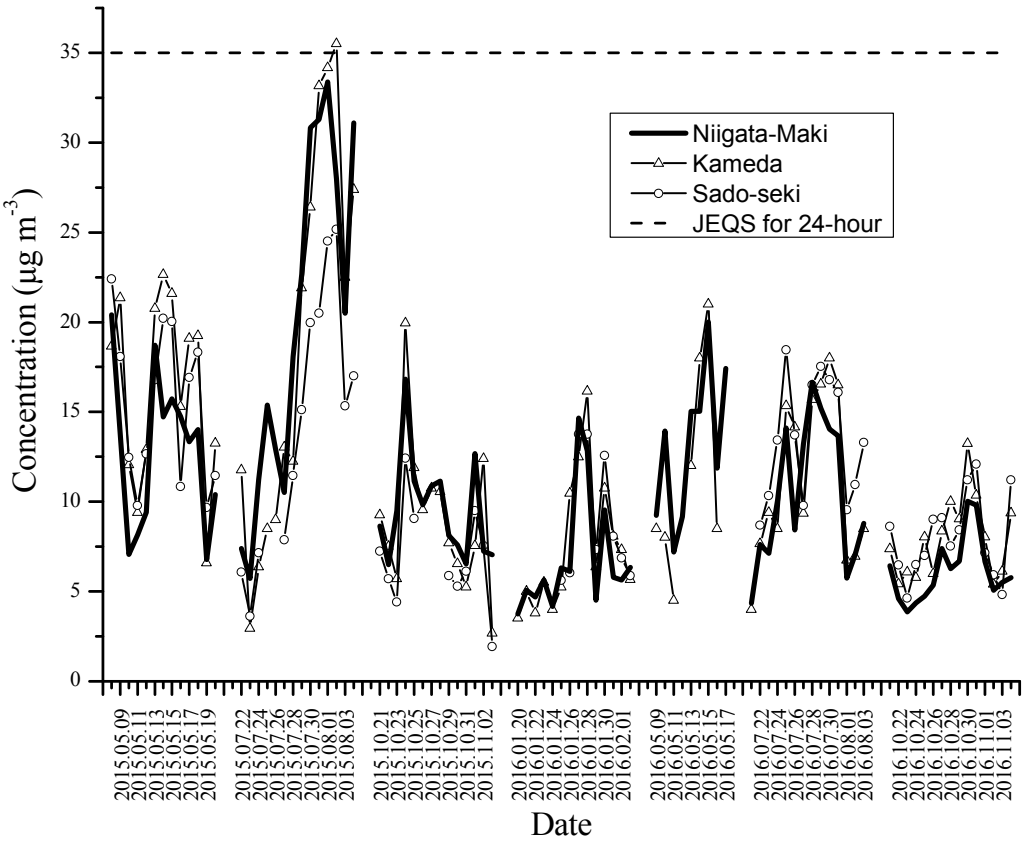

Fig. 3. Daily variations of $PM_{2.5}$ concentrations at Niigata-Maki, Kameda and Sado-seki site in Niigata.

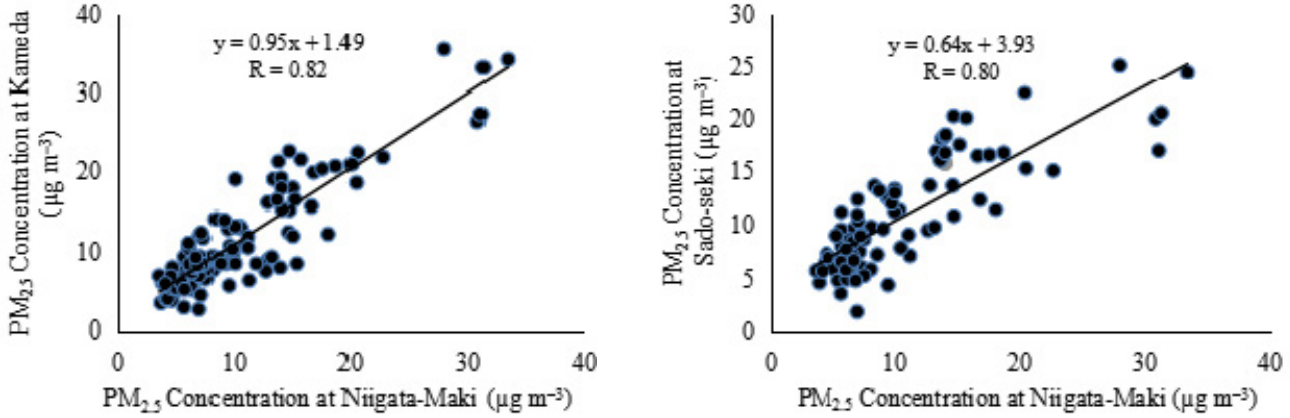

Fig. 4. The correlation plots of daily $PM_{2.5}$ mass concentrations at Niigata-Maki, Kameda and Sado-seki.

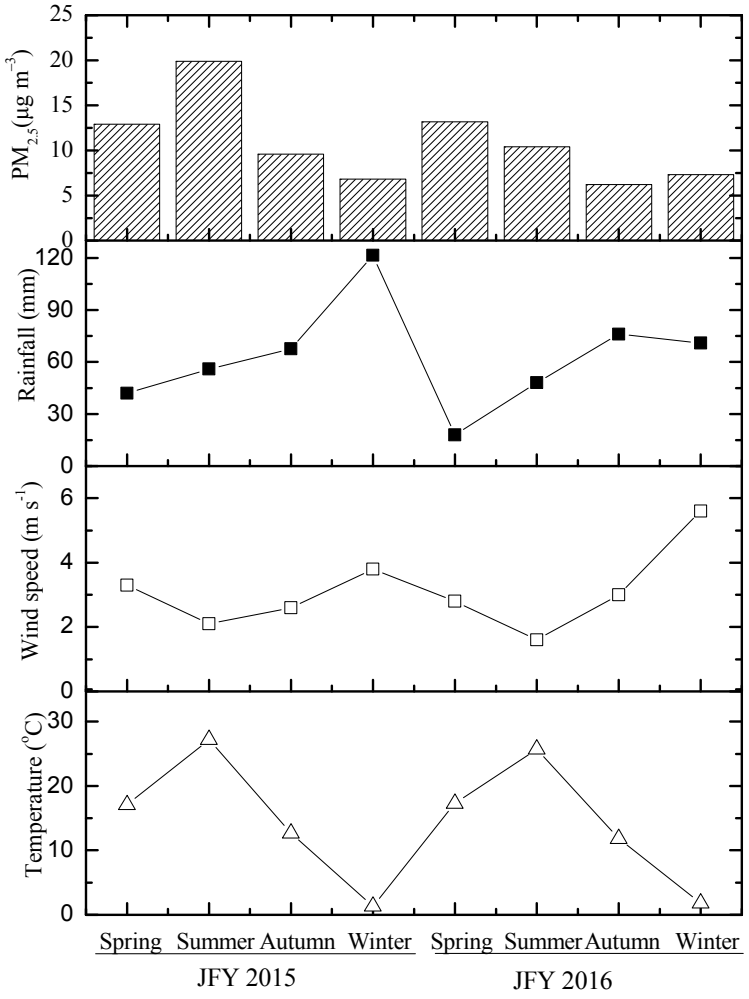

Fig. 5. Seasonal means of $PM_{2.5}$ mass concentration, rainfall, wind speed and temperature at the Niigata-Maki and the near meteorological station.

The mean contributions of nss-SO_4^{2-}, nss-K^+, nss-Ca^{2+}, nss-Mg^{2+} and nss-Cl^- to respect ionic concentrations in $PM_{2.5}$ were 97%, 94%, 34%, 14%, 2%, respectively. This result suggested that the major sources of SO_4^{2-} and K^+ in $PM_{2.5}$ were non-marine sources, and Cl^-, Mg^{2+} and Ca^{2+} were mainly originated from sea salts.

As shown in Table 4, the annual average concentrations of total water-soluble ions (TWSIs) in JFY 2015 and JFY 2016 were 6.5 μg m^{-3} and 3.8 μg m^{-3}, which accounted for 52.8% and 40.9% of $PM_{2.5}$ mass concentration in JFY 2015 and JFY 2016, respectively. Clear seasonal variations of TWSIs were observed at Niigata-Maki from May 2015 to

February 2017. The seasonal mean concentrations of TWSIs were in the order of summer > spring > winter > autumn (Table 4). The concentrations of sulfate (SO_4^{2-}) and ammonium (NH_4^+) were highest among all water soluble ions in $PM_{2.5}$. The annual means of SO_4^{2-} and NH_4^+ were 58.0% and 18.5% of the concentration of TWSIs in JFY 2015, 53.1% and 18.6% in JFY 2016, respectively. The higher concentrations of SO_4^{2-} and NH_4^+ were observed in spring and summer. NH_4^+ and SO_4^{2-} are known as tracer species of secondary aerosol, and the increased photochemical activity was one of the possible reasons for enhanced sulfate concentration during the period (Husain *et al*., 1990). Additionally, the annual mean molar ratio of NH_4^+ to SO_4^{2-} was 1.7 and 1.9 in JFY 2015 and 2016, respectively, the values were close to the molar ratio of NH_4^+ to SO_4^{2-} in $(NH_4)_2SO_4$ (2.0). This indicated that NH_4^+ and SO_4^{2-} were mainly from secondary aerosol $(NH_4)_2SO_4$.

Carbonaceous Species Analysis

Carbonaceous species in the atmosphere exist in three forms: organic carbon (OC), elemental carbon (EC), and carbonate carbon (CC). Because the ion balance of extract of $PM_{2.5}$ were satisfied with the required criteria, the contribution of carbonate to $PM_{2.5}$ was estimated to less than 5%. Therefore, total carbon (TC) in $PM_{2.5}$ was considered to be the sum of measured OC and EC (μgC) without pre-treatment of removal of carbonate.

As shown in Table 4, the annual mean concentrations of TC were 2.4 μgC m^{-3} and 2.1 μgC m^{-3}, which accounted for 19.5% and 22.6% of $PM_{2.5}$ concentrations in JFY 2015 and 2016, respectively. OC dominated over EC, and the annual mean OC/EC ratios were 2.6 and 3.2 in JFY 2015 and 2016, respectively. The ratio of OC/EC is often used as an indicator of the sources for the carbonaceous aerosol. We compared the annual mean OC/EC ratios between the Niigata-Maki site with those at some urban sites in Yokohama (Khan *et al*., 2010), Chiba (Ichikawa *et al*., 2015) and Kameda (MOEJ, 2016) in Japan. The annual mean OC/EC ratios at the Niigata-Maki (2.6 and 3.2 in JFY 2015 and 2016) were higher than those at the urban sites of Yokohama (1.9), Chiba (2.5) and Kameda (2.2). The Niigata-Maki site is classified as a rural site where there is no significant stationary source and low vehicular traffic. Because EC is considered as a tracer of diesel emission or fossil fuel combustion of stationary sources, the higher OC/EC ratio at the Niigata-Maki also represented the characteristics of a rural site.

The seasonal EC and OC concentrations were summarized in Table 4. EC concentration showed no strong seasonal variation. However, clear seasonal variation of OC was observed at the Niigata-Maki site. The seasonal mean concentrations of OC were in the order of spring > summer > autumn > winter during JFY 2015 and 2016. This result is similar to the results of some previous observational studies in Japan. For examples, the contribution of secondary formation, especially in summer, is more important for organic aerosols in Saitama, a suburban area of Tokyo (Bao *et al*., 2009). Moreover, the seasonal average contributions of secondary OC to total OC in $PM_{<2.1}$ were 60%, 75%, and 36% in spring, summer, and winter in Gunma Prefecture, a suburban area of Tokyo, respectively (Kumagai *et al*., 2010). The high contributions of secondary OC are attributable to high photochemical oxidant concentrations (> 100 ppb). The observed high OC concentrations in spring and summer may result from higher temperatures and more intense solar radiation, which provide favorable conditions for photochemical activity and secondary OC production (Khan *et al*., 2010).

Metallic Elements Analysis

In this study, 23 metallic elements (Al, Fe, Ni, Cr, Zn, Mn, Co, Cu, V, Ga, As, Se, Rb, Sr, Sc, Mo, Cd, Sb, Cs, Ba, Pb, Ag and Hg) in $PM_{2.5}$ were also measured during sampling period. The seasonal and annual mean concentrations and the crustal enrichment factor (EF) for each elements is summarized in Table 5. The EF has commonly been used as a first step in attempting to evaluate the strength of the crustal versus anthropogenic sources, defined as:

$$EF = ([Z]_{aerosol}/[Al]_{aerosol})/([Z]_{crust}/[Al]_{crust}), \quad (3)$$

where $[Z]_{aerosol}$ and $[Al]_{aerosol}$ are the target elements and aluminum concentrations in $PM_{2.5}$, and $[Z]_{crust}$ and $[Al]_{crust}$ are the reference concentrations of target elements and aluminum in crustal material (Alekseenko, 2014), respectively. If EF < 2, crustal soils are likely the predominant source for element, and if EF > 5 it suggests strong enrichment from non-crustal sources (Gao *et al*., 2002). The EF values in overall period (Mn, 1.65; Rb, 1.26; Sr, 0.43; Cs, 0.87 and Ba, 1.81) were lower, which suggests those elements were mainly from crustal sources. Since the EF of aluminum with respect to rubidium (Rb) is less than 1, aluminum is also mainly originated from crustal sources. The EFs for Ni, Cr, Se, Mo and Sb were obviously high (183, 116, 2445, 600 and 437) at Niigata-Maki site, which indicates that $PM_{2.5}$ is highly enriched by these metallic elements. Previous studies showed that the EFs of Ni, Cr, Se, Mo and Sb were higher (65, 32, 12300, 1370 and 20900) than other metallic elements in Tokyo. Furuta *et al*. (2005) suggested that Ni and Cr were originated from chemical industry sources, and Sb was from the combustion of plastic products and brake pad wear of automobiles. The EFs of Ni, Cr, Se were also high (55, 35, 6698) at the Hachimantai mountain range in northern Japan. This result suggested that Cr was originated from industrial sources, and the Se was from coal combustion or exhaust of vehicles (Kikuchi *et al*., 2010). These previous studies can be used for references to identify anthropogenic emission sources of the high EFs elements.

As shown in Table 5, the annual mean concentrations of a total 23 metallic elements were 702.3 ng m^{-3} (JFY 2015) and 279.2 ng m^{-3} (JFY 2016), which were 5.7% and 3.0% of the annual means of $PM_{2.5}$ at Niigata-Maki site, respectively. The concentrations of iron (Fe) and aluminum (Al) were highest among 23 metallic elements in $PM_{2.5}$. The major metallic elements Al and Fe to total metallic elements were accounted for 24.2% and 51.6% at Niigata-Maki site in JFY 2015, and 52.4% and 29.2% in JFY 2016, respectively. No obvious seasonal variation of metallic elements was

Table 5. Seasonal mean concentrations of metallic elements in $PM_{2.5}$ at Niigata-Maki. (N.D. = Not Detected).

Season		Al	Fe	Ni	Cr	Zn	Mn	Co
		ng m^{-3}	ng m^{-3}	ng m^{-3}	ng m^{-3}	ng m^{-3}	ng m^{-3}	ng m^{-3}
	Spring	283 ± 386	186 ± 175	3.45 ± 5.01	5.10 ± 2.07	N.D.	7.63 ± 8.26	0.12 ± 0.10
JFY	Summer	88.7 ± 39.6	144 ± 93.5	19.9 ± 18.3	6.47 ± 1.95	1.68 ± 6.30	4.37 ± 2.40	0.29 ± 0.70
2015	Autumn	71.6 ± 45.8	77.6 ± 26.9	22.5 ± 24.5	5.01 ± 1.47	N.D.	2.24 ± 1.03	0.22 ± 0.23
	Winter	235 ± 157	1037 ± 1486	125 ± 195	263 ± 438	70.0 ± 99.9	14.6 ± 18.7	3.01 ± 4.59
Annual mean		167 ± 220	364 ± 836	43.5 ± 108	71.2 ± 243	18.2 ± 57.9	7.19 ± 11.1	0.93 ± 2.59
	Spring	171 ± 29.8	36.8 ± 22.4	6.15 ± 6.38	4.08 ± 1.61	5.74 ± 13.0	1.73 ± 1.22	0.04 ± 0.04
JFY	Summer	70.8 ± 71.5	48.9 ± 35.5	7.12 ± 6.11	5.85 ± 2.68	27.4 ± 59.3	2.17 ± 1.32	0.10 ± 0.16
2016	Autumn	262 ± 227	136 ± 64.2	7.65 ± 7.06	4.19 ± 2.44	N.D.	4.50 ± 2.45	0.04 ± 0.02
	Winter	59.5 ± 29.0	91.9 ± 37.8	3.08 ± 6.64	5.56 ± 2.20	7.46 ± 19.7	1.69 ± 1.27	0.32 ± 0.69
Annual mean		144 ± 152	82.4 ± 59.05	6.06 ± 6.64	4.93 ± 2.36	10.9 ± 33.1	2.63 ± 2.05	0.13 ± 0.36
EF Value		0.79[a]	2.45	183	116	22.6	1.65	9.19

Season		Cu	V	Ga	As	Se	Rb	Sr
		ng m^{-3}	ng m^{-3}	ng m^{-3}	ng m^{-3}	ng m^{-3}	ng m^{-3}	ng m^{-3}
	Spring	3.03 ± 1.59	3.33 ± 3.22	0.51 ± 0.49	1.46 ± 1.06	0.92 ± 0.60	0.64 ± 0.65	1.14 ± 1.49
JFY	Summer	4.80 ± 2.43	4.66 ± 3.40	0.79 ± 1.84	0.93 ± 1.10	1.05 ± 0.78	0.30 ± 0.16	1.11 ± 0.68
2015	Autumn	1.81 ± 0.62	0.52 ± 0.16	0.51 ± 0.48	0.59 ± 0.47	0.34 ± 0.19	0.30 ± 0.10	0.46 ± 0.24
	Winter	7.78 ± 10.5	1.67 ± 1.85	0.48 ± 0.25	0.68 ± 0.48	0.31 ± 0.33	0.33 ± 0.17	0.88 ± 0.40
Annual mean		4.38 ± 5.82	2.53 ± 2.91	0.57 ± 1.00	0.91 ± 0.88	0.65 ± 0.61	0.39 ± 0.36	0.89 ± 0.85
	Spring	1.58 ± 1.47	2.42 ± 2.76	0.08 ± 0.10	0.70 ± 0.44	0.38 ± 0.25	0.21 ± 0.15	0.29 ± 0.24
JFY	Summer	3.33 ± 2.85	1.64 ± 0.92	0.51 ± 1.25	0.61 ± 0.33	0.52 ± 0.29	0.17 ± 0.13	0.80 ± 0.69
2016	Autumn	2.37 ± 1.81	0.38 ± 0.24	1.49 ± 0.57	0.46 ± 0.57	0.29 ± 0.22	0.29 ± 0.16	1.14 ± 0.93
	Winter	1.16 ± 0.61	0.38 ± 0.17	0.37 ± 0.22	0.39 ± 0.45	0.26 ± 0.20	0.20 ± 0.17	0.47 ± 0.39
Annual mean		2.14 ± 2.00	1.13 ± 1.56	0.61 ± 0.53	0.54 ± 0.46	0.36 ± 0.26	0.22 ± 0.15	0.71 ± 0.71
EF Value		20.4	4.27	9.36	11.07	2445	1.26	0.43

Season		Sc	Mo	Cd	Sb	Cs	Ba	Pb
		ng m^{-3}	ng m^{-3}	ng m^{-3}	ng m^{-3}	ng m^{-3}	ng m^{-3}	ng m^{-3}
	Spring	0.78 ± 0.38	5.87 ± 19.5	0.44 ± 0.28	1.08 ± 0.56	0.07 ± 0.07	6.17 ± 6.05	8.76 ± 4.80
JFY	Summer	0.68 ± 0.57	0.68 ± 0.31	0.20 ± 0.16	1.06 ± 0.90	0.03 ± 0.02	9.85 ± 26.2	6.06 ± 4.60
2015	Autumn	0.49 ± 0.25	0.63 ± 0.20	0.09 ± 0.04	5.67 ± 6.90	0.02 ± 0.01	6.13 ± 9.88	7.32 ± 13.5
	Winter	0.95 ± 0.68	2.14 ± 2.96	0.13 ± 0.16	1.37 ± 1.00	0.02 ± 0.02	3.85 ± 3.55	4.31 ± 3.64
Annual mean		0.72 ± 0.60	2.27 ± 9.55	0.21 ± 0.22	2.32 ± 3.90	0.03 ± 0.03	6.51 ± 14.3	6.57 ± 7.75
	Spring	N.D.	0.28 ± 0.19	0.13 ± 0.10	0.75 ± 0.61	0.02 ± 0.03	1.32 ± 0.99	3.66 ± 3.27
JFY	Summer	N.D.	0.49 ± 0.24	0.11 ± 0.07	0.94 ± 0.47	0.01 ± 0.01	7.81 ± 17.5	3.65 ± 2.26
2016	Autumn	1.09 ± 2.02	32.2 ± 31.0	0.55 ± 1.10	0.63 ± 0.60	0.01 ± 0.01	10.2 ± 9.19	4.04 ± 3.57
	Winter	0.23 ± 0.73	0.17 ± 0.12	0.09 ± 0.10	2.74 ± 4.15	0.01 ± 0.02	3.70 ± 1.68	4.62 ± 5.39
Annual mean		0.37 ± 1.21	9.51 ± 21.8	0.24 ± 0.62	1.26 ± 2.25	0.01 ± 0.02	6.11 ± 10.4	4.01 ± 3.71
EF Value		12.8	600	59.7	437	0.87	1.81	23.7

The values after "±" denote standard deviations based on daily mean concentrations.

[a] EF of aluminum is calculated by $([Z]_{aerosol}/[Rb]_{aerosol})/([Z]_{crust}/[Rb]_{crust})$.

The concentrations of Ag and Hg were under detection limits during sampling periods, and thus they were not shown in Table 5.

observed, but we found a remarkably high concentration event of Fe, Ni and Cr in winter JFY 2015. These metallic elements were recommended as markers for the metal processing industry, especially for steel works (Chen *et al*., 2014). The waste incineration was also a source of Ni and Cr (Reimann *et al*., 1998).

$PM_{2.5}$ Mass Balance

Summation of determined major chemical components (SO_4^{2-}, NO_3^-, Cl^-, NH_4^+, Na^+ and EC) and estimated fraction (Organic carbon matter (OCM) and soil dust) were compared with $PM_{2.5}$ mass concentration to evaluate whether the mass balance discrepancy was significant. The following equation was used to estimate OCM including O, H, N compounds:

$$OCM = k\,(OC_m - OC_b) \quad (4)$$

where OCM is organic carbon matter; k is adjustment factor to account for non-carbon organic matter (1.4) (Bell

et al., 2007); OC_m is measured organic carbon; OC_b is organic carbon for blank filters. Soil dust was estimated from the measured concentrations of Al, Mg, K, Ca, Fe, and the estimated concentration of Si. The silicon concentration was estimated from the average mass ratio of Si to Al in the earth's crust as Si = 3.41Al (Mason, 1966), the concentration of soil dust was calculated with the following equation (Hueglin *et al*., 2005).

$$\text{Soil dust} = 1.89\text{Al} + 1.66\text{Mg} + 1.21\text{K} + 1.40\text{Ca} + 1.43\text{Fe} + 2.14\text{Si} \quad (5)$$

Fig. 6 shows the mass balance between the $PM_{2.5}$ mass and the sum of the aerosol chemical components. The annual means $PM_{2.5}$ mass was 6.2% and 17.0% larger than the sums of the aerosol chemical components in JFY 2015 and 2016, respectively. The discrepancy between the $PM_{2.5}$ mass and the sums of the aerosol chemical components varies among different seasons, and the $PM_{2.5}$ mass exceeded maximum 30.8% in spring JFY 2016. On the other hand, the $PM_{2.5}$ mass was maximum 29.5% lower than the sum of the aerosol chemical components in winter JFY2015. This can be explained by the remarkably higher concentration of Fe. The EF value of Fe was 7.56 in winter JFY 2015, which implies that a significant portion of Fe was originated from anthropogenic sources. Since all of Fe measured concentrations were calculated soil dust by the Eq. (5), the portion of soil dust was irregularly higher, and thus the sum of the aerosol chemical component exceeded the $PM_{2.5}$ mass in winter JFY 2015. Previous studies suggested that the mass balance discrepancy and its seasonal shift may be due to a combination of aerosol water content retained on the conditioned filters, and volatilization losses of $PM_{2.5}$ (Hering *et al*., 1999; Pang *et al*., 2002).

Major Components of $PM_{2.5}$

Fig. 7 shows annual average concentrations and annual average contributions of major components in $PM_{2.5}$ at Niigata-Maki site. The same data at Kameda, Chiba and Japan national-average are also shown as references. As shown in Fig. 7(b), water-soluble ions, OC and EC, which are major components of $PM_{2.5}$, accounted for 52.8%, 14.5% and 5.4% of the annual means $PM_{2.5}$ mass concentration at Niigata-Maki site in JFY 2015, and accounted for 40.8%, 17.3% and 5.3% in JFY 2016, respectively. The sum of NO_3^-, SO_4^{2-} and NH_4^+ accounted for 82.0% and 80.6% of the water-soluble ions in JFY 2015 and 2016, respectively. The "Others" fraction is defined as $PM_{2.5}$ mass concentration minus the sum of water-soluble ions, EC and OC concentrations. The others accounted for 27.3% and 36.6% of the annual means $PM_{2.5}$ mass concentration in JFY2015 and 2016, respectively. This fraction is assumed to contain trace elements, organic matters other than carbon (OM), crustal elements of soil dust and analytical uncertainties of the measurement. OM was estimated by Eq. (4), OM = OCM – OC. Soil dust was estimated by Eq. (5). The annual sum of OM and soil dust accounted for 69.4% of the "Others" fraction, as shown in Fig. 6. These results showed that SO_4^{2-}, NO_3^-, NH_4^+, OCM, EC and crustal elements were the major chemical components of $PM_{2.5}$ in Niigata.

We compared the mass concentration and the contributions of major components of $PM_{2.5}$ among Niigata-Maki, Kameda (MOEJ, 2016), Chiba (Ichikawa *et al*., 2015) and Japan national average (MOEJ, 2016). As shown in Fig. 7(a), annual

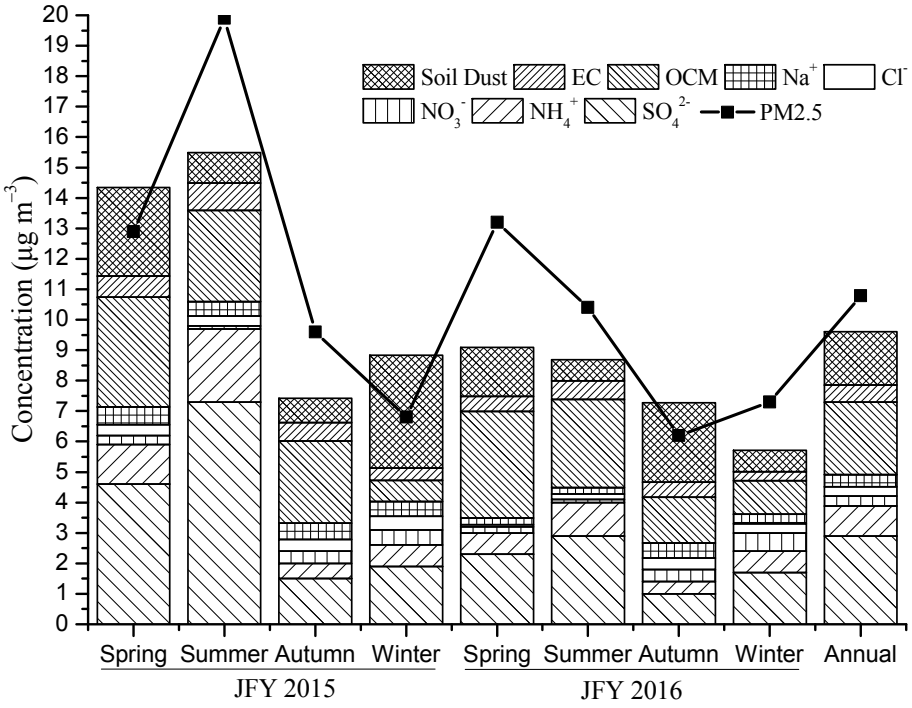

Fig. 6. Seasonal and annual discrepancy between the $PM_{2.5}$ mass and the sums of the aerosol chemical components at Niigata-Maki. Annual is the average concentration of JFY2015 and 2016.

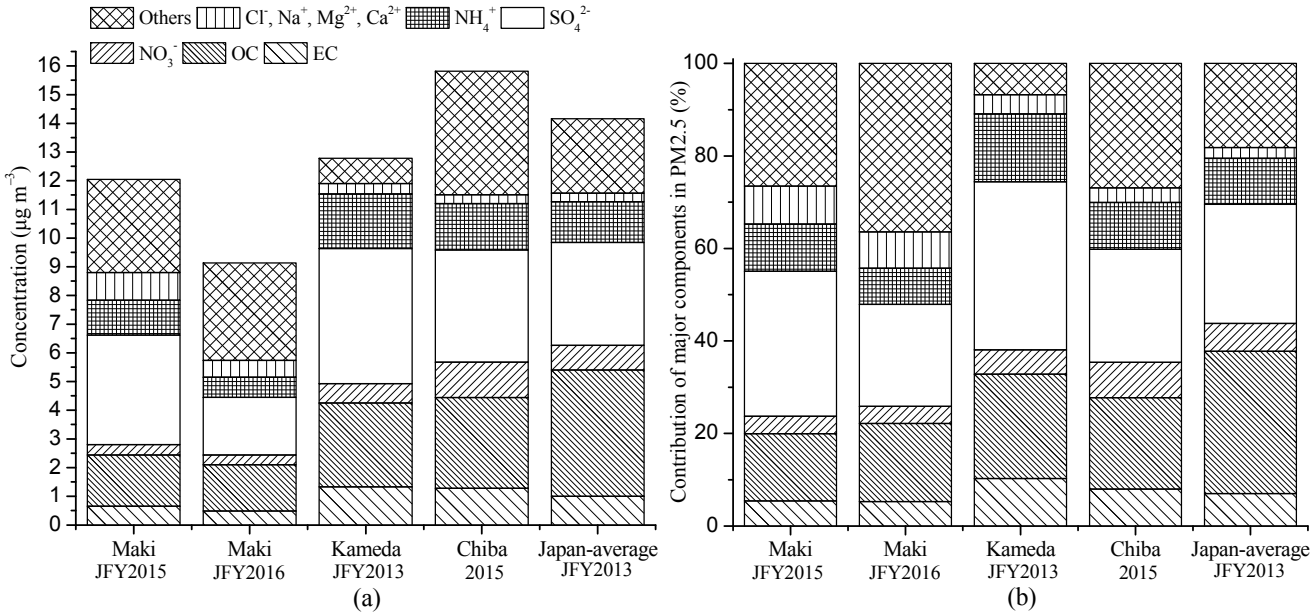

Fig. 7. (a) Annual average concentrations and (b) Annual average contributions of major components in $PM_{2.5}$ at Niigata-Maki (JFY 2015 and 2016), Kameda (JFY 2013), Chiba (JFY 2015) and the Japan national average (JFY 2013). Others was calculated by subtraction of the $PM_{2.5}$ mass concentrations from the sum of water-soluble ions, EC and OC concentrations.

mean mass concentration of $PM_{2.5}$ at Niigata-Maki site was lower than Kameda, Chiba and Japan national average, and Chiba annual mean exceeded the annual JEQS mass concentration (15 μg m^{-3}). These results are probably due to respective site locations that Niigata-Maki is a rural site and Kameda is an urban site in Niigata, and that the Chiba site is located in Tokyo metropolitan area.

As shown in Fig. 7(b), the ratio of total sea salt related ions of Cl^-, Na^+, Mg^{2+} and Ca^{2+} to the $PM_{2.5}$ mass at Niigata-Maki (8.2% in JFY 2015, 7.8% in JFY 2016) was obviously higher than Kameda (4.1%), Chiba (3.1%) and Japan national average (2.3%), which is mainly due to the site location being close to the coast of the Sea of Japan. The ratios of EC to the $PM_{2.5}$ mass at Niigata-Maki (5.4% in JFY 2015, 5.3% in JFY 2016) were lower than at Kameda (10.3%), Chiba (8.0%) and Japan national average (7.0%), and the OC/EC ratios of Niigata-Maki (2.6 in JFY 2015, 3.2 in JFY 2016) were higher than Kameda (2.2), Chiba (2.5), which may be due to fewer traffic emission source near Niigata-Maki site. Since EC is an indicator of primary emission, diesel vehicle exhaust is probably the main source of EC in urban areas (Bao *et al.*, 2016). The ratios of NO_3^- to $PM_{2.5}$ mass at Niigata-Maki were obviously lower than Kameda and Chiba which also may be due to fewer traffic emission sources. The above differences showed that the contribution of vehicle source to $PM_{2.5}$ would be lower at the Niigata-Maki site.

Source Apportionment of $PM_{2.5}$ from PMF Analysis

EPA PMF 5.0 was used to identify the potential sources of $PM_{2.5}$. The aim of PMF model is to minimize the function *Q*. Missing values were replaced by the median concentration of a given species, with an uncertainty of four times the median (Brown *et al.*, 2015). Values below method detection limit (MDL) are retained and related uncertainties are set at 5/6 of detection limit values. For values greater than the MDL, the calculation is based on a user provided fraction of the concentration and MDL, and the error fraction was suggested as 10% by the previous study of Paatero (2007). Uncertainty is defined as:

$$\text{Uncertainty} = \sqrt{(\text{Error Fraction} \times \text{concentration})^2 + (0.5 \times \text{MDL})^2} \quad (6)$$

The number of factors to be chosen will depend on the user's understanding of the sources impacting samples, number of samples, sampling time resolution, and species characteristics. We run the PMF5.0 with moving the factors from two to seven, the decrease of Q/Qexpected is illustrated from 13.8 to 7.9, as well as a smaller decrease with moving from six to seven factors (8.4–7.9). When the changes in Q values become smaller than the increase of factors, it can suggest that there may be too many factors being fit (Brown *et al.*, 2015; Liu *et al.*, 2017). This result indicated that six factors may be the optimal solution.

The error estimation results of classical bootstrap (BS), displacement of factor elements (DISP), and bootstrap enhanced by displacement (BS-DISP), which is due to the small size of the data set and limited number of factors. The source apportionment results were generally stable at six factors, with all factors mapped in BS in 100% of runs except for the vehicle and industrial source factors (mapped on 85% and 81% of runs), mapping over 80% of the factors indicates that the BS uncertainties can be interpreted and the number of factors may be appropriate (PMF 5.0 User Guide, 2016). No swaps occurred with DISP also showed that the solution is stable, and all BS-DISP runs were

successful. $PM_{2.5}$ source apportionment was characterized by the following six factors, as shown in Fig. 8, and the contributions of each source to the $PM_{2.5}$ mass was shown in Fig. 9. Each factor could be characterized as follows.

Factor 1 was characterized by high positive loading of Cl^- (78.2%), NO_3^- (40.9%), Na^+ (64.2%), Mg^{2+} (71.1%) and Ca^{2+} (28.6%), which were mainly from sea salt. This result is consistent with the correlation result that Na^+ was significantly correlated with Cl^-, Mg^{2+} and Ca^{2+}. The contributions of nss-SO_4^{2-}, nss-K^+, nss-Ca^{2+}, nss-Mg^{2+} and nss-Cl^- in $PM_{2.5}$ calculated from the Eq. (2) also showed that 98% of Cl^-, 86% of Mg^{2+} and 66% of Ca^{2+} were from marine sources. Thus, the factor 1 was identified as sea salt, and its contribution to $PM_{2.5}$ was 10.2% as shown in Fig. 9.

Factor 2 was characterized by high positive loading of OC (85.9%), EC (52.9%) and K^+ (81.5%), which are generally considered as indicators of biomass burning, and K^+ is a widely used tracer of biomass burning source (Almeida *et al*., 2015; Yao *et al*., 2016). Thus, the factor 2 was identified as biomass combustion, and its contribution to $PM_{2.5}$ was 18.9%.

Factor 3 was characterized by high positive loading of Al (65.1%), Ga (54.8%), Sr (57.9%) and Ba (74.8%), which were mainly originated from crustal soil. As previously mentioned, the elements of EF < 2 suggest mainly natural crustal source origin, and those of EF > 5 suggest strong enrichment by non-crustal sources (Gao *et al*., 2002). The mean EF values of these elements during overall period were very low (Al, 0.79; Ba, 1.81; and Sr, 0.43). This suggests that these elements are mainly originated from natural sources and mineral matter. It was also reported that trace elements of Ga and Sr are originated from re-suspension of road dust (Amato *et al*., 2012). Thus, the factor 3 was identified as soil dust, and its contribution to $PM_{2.5}$ was 13.2%.

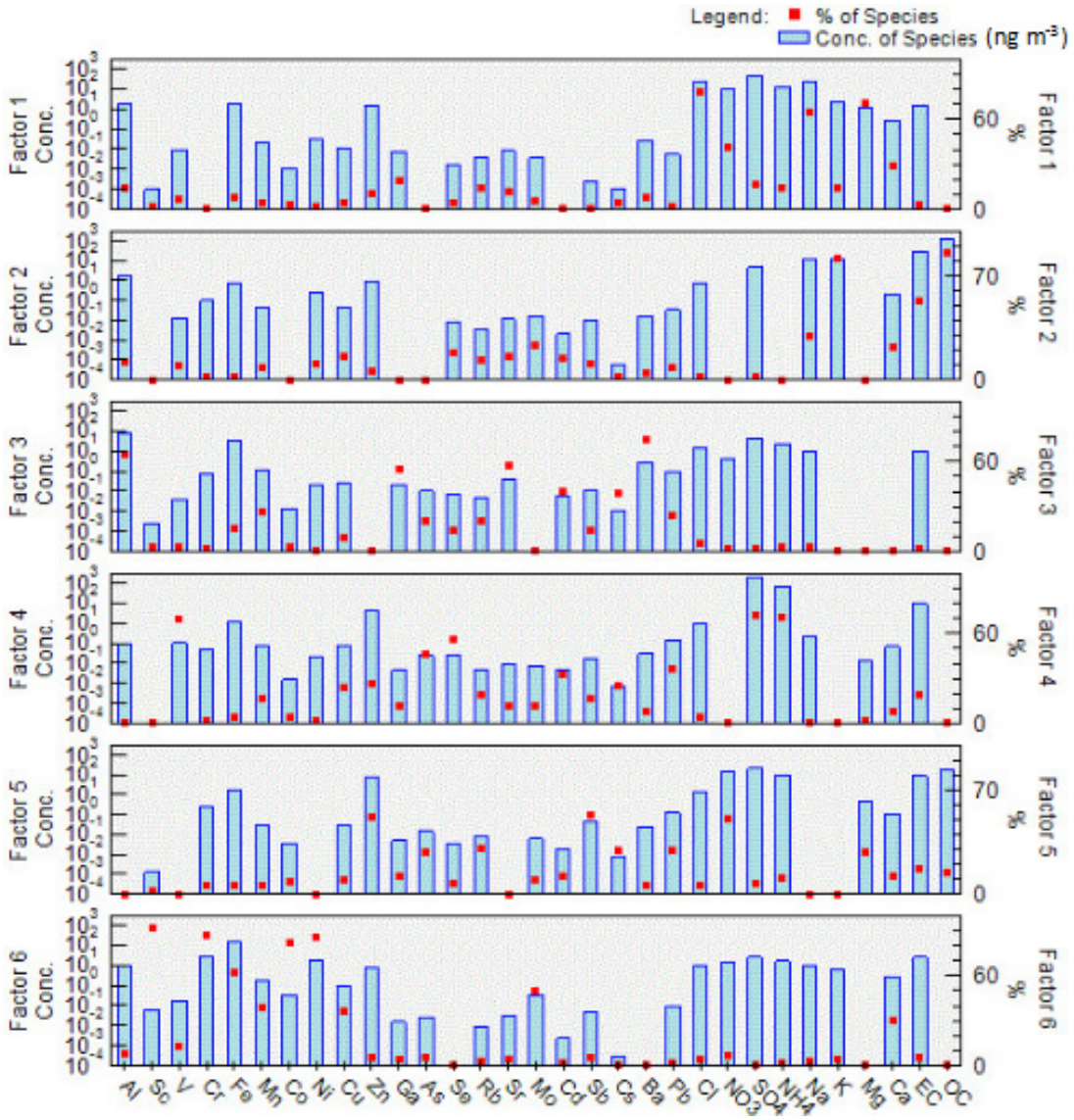

Fig. 8. Six factors obtained by using the PMF 5.0 model for each source category at Niigata-Maki: (Factor 1) sea salt, (Factor 2) biomass combustion, (Factor 3) soil dust, (Factor 4) secondary aerosol, (Factor 5) vehicular traffic, and (Factor 6) industrial activity.

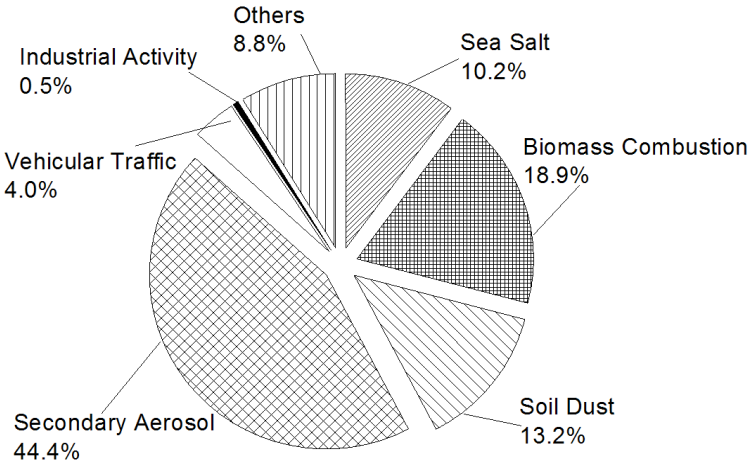

Fig. 9. The annual mean contribution of each source to $PM_{2.5}$ estimated from PMF analysis at Niigata-Maki.

Factor 4 was characterized by high positive loading of major components of SO_4^{2-} (71.7%) and NH_4^+ (71.1%), and their typical source is secondary aerosol such as $(NH_4)_2SO_4$. Factor 4 was also represented by the high positive loading of metallic elements of V (69.4%), As (46.2%), Se (56.2%) and Pb (35.6%). V is a marker element of oil combustion (Okuda *et al.*, 2006), and As, Se and Pb are the typical anthropogenic sources of coal combustion (Reimann *et al*., 1998; Wahlin *et al*., 2006). Many PMF source apportionment studies have reported a relationship between $(NH_4)_2SO_4$ and particulate matter components of combustion origin, such as heavy metals (Kim *et al.*, 2004). This is likely associated with SO_2 emissions from oil or coal-burning power plants forming secondary sulfate and reacting with gaseous NH_3 from a variety of sources. Thus, the factor 4 was identified as secondary aerosol and possibly associated with coal or oil combustion processes, and its contribution to $PM_{2.5}$ was 44.4%.

Factor 5 was characterized by high positive loading of Zn (52.3%), Sb (53.1%), NO_3^- (50.8%), As (28.6%) and Pb (29.2%), and their typical source is vehicular traffic. Zn is a marker element of tire wear (Wahlin *et al*., 2006), and Sb is known as a tracer of brake wear dusts (Iijima *et al*., 2008, Iijima *et al*., 2009). Mn and As are also emitted from re-suspension of road traffic-generated particles (Fabretti *et al*., 2009). Pb is originated from tire dust or fuel combustion of vehicle (Smichowski *et al*., 2008). Vehicular traffic is also a significant source of gaseous precursors (NO_x) and formed secondary aerosol of nitrate (de Gouw *et al*., 2009). Thus, the factor 5 was identified as vehicular traffic, and its contribution to $PM_{2.5}$ was 4.0%.

Factor 6 was characterized by high positive loading of Sc (92.9), Co (81.9%), Fe (62.9%), Cr (87.3%) Ni (86.5%), Cu (36.7%) and Mo (50.1%), which were possibly attributed to industrial activities. The common anthropogenic sources of Co, Cr, Ni, Cu and Fe include steel works and smelters. They are considered as markers for metal processing industry, especially for steel works (Reimann *et al*, 1998; Chen *et al*., 2014). Co and Ni are possibly originated from crude oil processing in refineries (Speight, 2014). Waste incineration is also a source of Ni and Cr (Reimann *et al*, 1998). Thus, the factor 6 was identified as industrial activity, and its contribution to $PM_{2.5}$ was 0.5%.

The PMF analysis demonstrated that the major sources of $PM_{2.5}$ at the Niigata-Maki site were identified to be sea salt, biomass combustion, soil dust and secondary aerosol. Comparing with previous studies in western Japan, the major sources of $PM_{2.5}$ in an industrial area of Hyogo Prefecture, located in the southern-central region of Honshu, were identified to be secondary sulfates (28.9%), vehicular traffic (20.8%), steel mills (7.8%), and secondary chloride and nitrate (7.0%) (Nakatsubo *et al*., 2014). The major sources of $PM_{2.5}$ in Okinawa were identified to be coal combustion (32.6%), secondary species (28.5%), sea salt and nitrate (19.1%), oil combustion (12.8%), and soil dust (7.0%) (Shimada *et al*., 2015). The high contribution of secondary aerosol was common between western Japan and our study, whereas low contribution of vehicular traffic and high contribution of biomass combustion in our study showed unique characteristics in the coast of the Sea of Japan. Indeed, our identified sources included both local and long range origin. In the next section, the significant origin area of the major sources of $PM_{2.5}$ will be identified by the PSCF analysis.

Emission Regions of $PM_{2.5}$ Major Sources by PSCF Analysis

We performed the PSCF analysis to identify the preferred atmospheric transport pathways from sources to receptors by the Meteoinfo1.4.3: GIS-based software that uses various trajectory statistical analysis methods to identify potential sources from long-term air pollution measurement data (Wang *et al.*, 2009). 72-h backward trajectories were obtained by using the Meteoinfo1.4.3 model from the Global Data Assimilation System (GDAS) meteorological data (ftp://gus.arlhq.noaa.gov./). We used PSCF to estimate the back trajectories at arrival heights of 500, 1000, and 1500 m, and three-day back trajectories were used to calculate the PSCF values for 1° × 1° grid cells computed for arrival heights of 500, 1000, and 1500 m for each of the 106 daily mean samples. The studying field is from 30 to 50°N, and 120 to 150°E, which includes more than 95% of area covered by all the paths. Regions with PSCF values

ranging from 0.5 to 1 were designated as probable source regions for each factor during the study period. The potential source regions of the four major sources identified PMF analysis are shown in Fig. 10. The detailed discussions for respective sources are shown below.

Sea Salt

Sea salt was characterized as major components of Cl^-, Na^+, Mg^{2+} and Ca^{2+} by PMF analysis, Niigata-Maki station lies on the coast of the Sea of Japan, 1 km from the seashore, and thus, the high value PSCF plots suggested that Sea of Japan was the main source area of sea salt, as shown in Fig. 10(a).

Biomass Combustion

Biomass combustion source was characterized as major components of OC, EC and K^+ by PMF analysis. As shown in Fig. 10(b), the high value PSCF plots suggested that local area in Niigata, southwest Japan, northeast China and Korea were the potential source areas. The biomass combustion emissions in the NEA are generally from agricultural waste burning after barley and wheat harvest (between late spring and early summer) and rice harvest (in the autumn) (Zang, 2015). Biomass burning activity in the NEA during these period were also estimated using a fire spot database, and the fire spots data are provided by the Fire Information for Resource Management System (FIRMS) (https://firms.modaps.eosdis.nasa.gov/firemap/), the satellite image in Fig. S1 showed dense hot spots appeared in northeast China in autumn during the sampling period. To better identify the potential sources of aerosols originating from these regions, we used seasonal fire spots to compare with the autumn biomass combustion PSCF plots (Fig. 11). The high dense regions of hotspot in autumn JFY 2015 and 2016 corresponded to high PSCF areas. These results showed that the major source of biomass combustion was from northeast China in autumn, and local area in Niigata and southwest Japan were the main source areas in the other seasons. Our previous study also showed high concentration episode of water insoluble organic carbon and EC in precipitation that is synchronized with high number of fire spots in the NEA, which implies considerable contribution of biomass combustion in spring and autumn (Huo *et al.*, 2016).

Soil Dust

Crustal soil source was characterized as key elements of Al, Ga, Sr and Ba by PMF analysis. As shown in Fig. 10(c), the high value PSCF plots suggested that local area in Niigata, northeast China, Korea and the Sea of Japan were

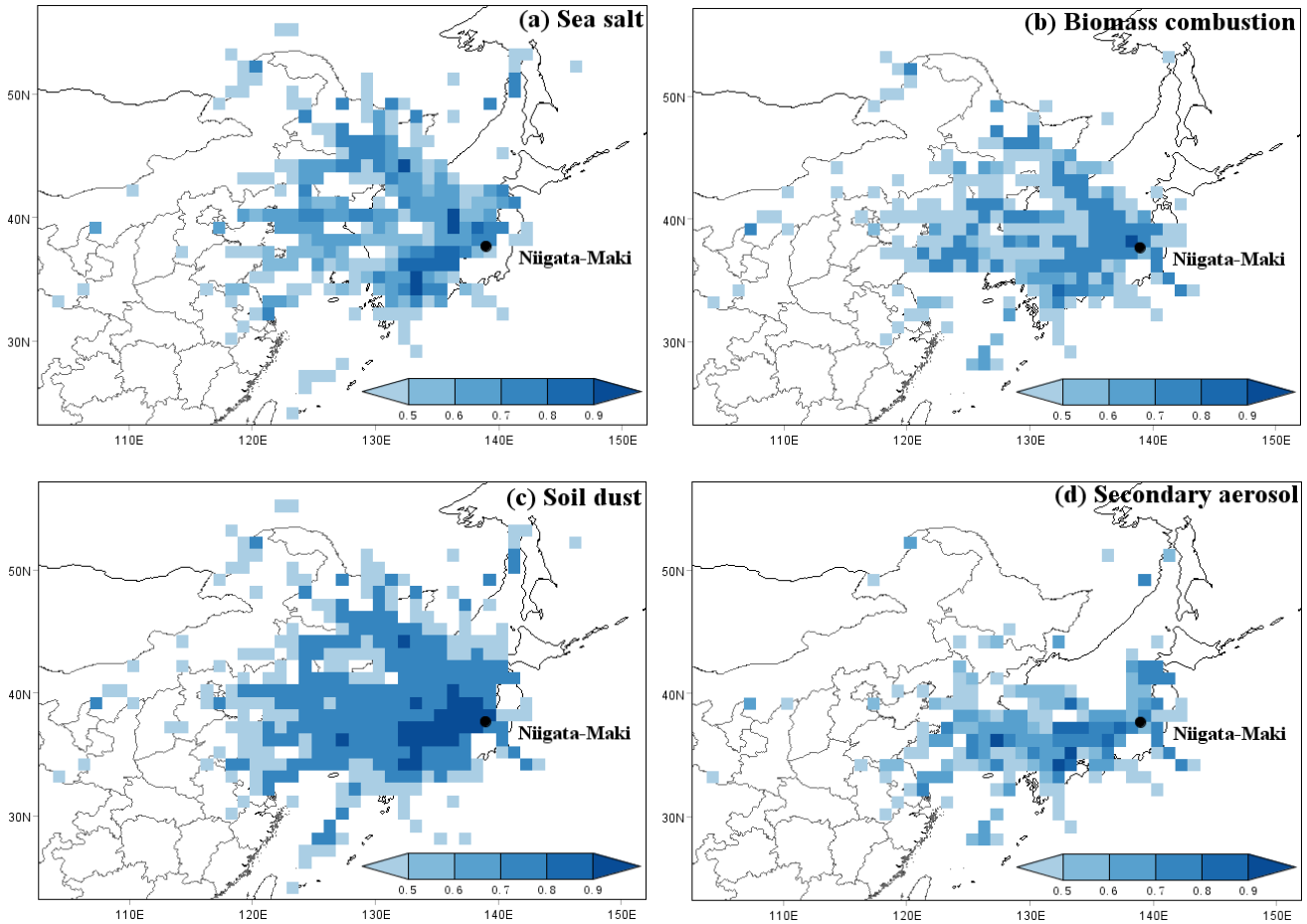

Fig. 10. Potential source regions by using PSCF analysis for annual mean: (a) sea salt, (b) biomass combustion, (c) soil dust, and (d) secondary aerosol.

the potential sources considering all seasons. When we focus on the seasonal soil dust PSCF plots in winter (Fig. 12), the major source area of soil dust was northeast China. For the other seasons, contributions of local area in Niigata and the Sea of Japan were more remarkable.

Secondary Aerosol

Secondary aerosol was characterized as major components SO_4^{2-} and NH_4^+ by PMF analysis. As shown in Fig. 10(d), the high value PSCF plots suggested that southwest Japan and Korea were the potential sources. The PMF source apportionment results showed a relationship between $(NH_4)_2SO_4$ and combustion origin. This was likely associated with SO_2 emissions from oil or coal burning power plants. Fig. S2 show that the thermal power plants are concentrated in the southwest of Japan and Tokyo metropolitan area. Coal or oil burning factories and volcanoes were also the potential source of SO_4^{2-} in Japan, Itahashi *et al*. (2017) revealed that the contribution of SO_4^{2-} originated from volcanoes is 28.7% in summer. The concentrations of SO_4^{2-} and NH_4^+ were obviously high in summer as shown in Table 4, when the Pacific high covers the mainland in Japan and the air mass is usually transported along the ridge of the Pacific high. Moreover, the central mountains in Japan seem to hinder transportation of air pollutants from Tokyo metropolitan area. In addition, for the summertime contribution of sulfate aerosol, many previous observation and numerical model simulation studies showed the large contribution from the Asian continent, especially China. For example, Aikawa *et al*. (2010) revealed the strong gradient of sulfate from west to east by comparing the observational data in several stations. This is the suggestion of long-range transport of sulfate aerosol over the Asian continent. The numerical modeling revealed that central China was the main SO_4^{2-} source region in China (Kajino *et al*., 2011; Itahashi *et al*., 2017). In Japan, the concentration of SO_4^{2-} was highest in summer and followed in spring, which the long range transportation of SO_4^{2-} from central China also had the great impact on sulfate concentration during the two seasons (Itahashi *et al*., 2017). Ikeda *et al.* (2015) revealed

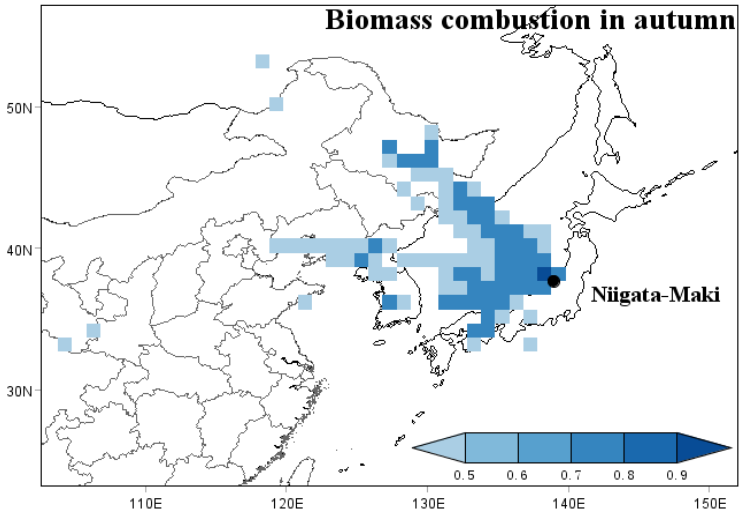

Fig. 11. Potential source regions of biomass combustion in autumn by using PSCF analysis at Niigata-Maki.

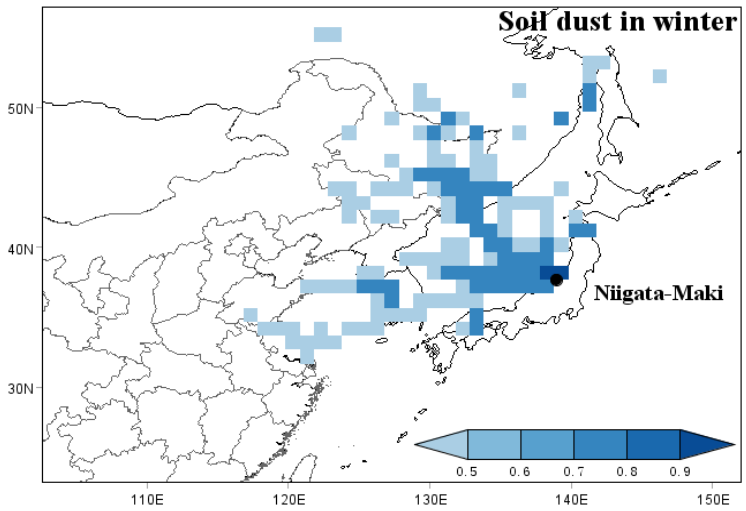

Fig. 12. Potential source regions of soil dust in winter by using PSCF analysis at Niigata-Maki.

that the relative contribution of China to the annual mean $PM_{2.5}$ concentration was estimated to be 50–60% in western Japan. Comparing with the previous studies showed that southwest Japan was the important source area contributing to secondary aerosol, which included local and long-range transport sources.

Table 4 also shows that the concentrations of SO_4^{2-} and NH_4^+ were higher in spring, and the back trajectory analysis results showed that the origins of the air masses arriving at Niigata-Maki were mainly from two regions (central China and southwest Japan), as shown in Fig. S3. Comparing with the above discussion on sulfate aerosol, which central China and southwest Japan were the important source areas in Japan. Therefore, it is also probable that the two regions had a great impact on secondary aerosols in Niigata during spring.

The above results showed that the major sources of secondary aerosol and sea salts are domestic in southwest Japan and the Sea of Japan, whereas the sources of biomass combustion and soil dust in specific seasons are long range transportation from the NEA. Comparing with previous studies of PSCF analysis in urban area of western Japan (Nakatsubo *et al*., 2014) and in remote area of southwestern Japan (Shimada *et al*., 2015), this study showed a large domestic contribution of southwest Japan for secondary aerosol, while a larger contribution of the NEA was observed in previous studies. Moreover, significant contribution of biomass combustion originating from local or long range transportation was observed on the coast of the Sea of Japan. This study showed the regional characteristics of $PM_{2.5}$ sources in eastern Japan.

CONCLUSION

In this research, a field observation study including seasonal intensive measurement of $PM_{2.5}$ was conducted from May 2015 to February 2017 at Niigata-Maki station in Niigata, eastern Japan. The annual mean mass concentrations of $PM_{2.5}$ were 12.3 μg m^{-3} (JFY 2015) and 9.3 μg m^{-3} (JFY 2016). Daily mean concentrations of $PM_{2.5}$ ranged from 4.2 μg m^{-3} to 33.4 μg m^{-3} at Niigata-Maki station during observation period, which were lower than Japanese Environmental Quality Standard for $PM_{2.5}$ (35 μg m^{-3} for daily average). $PM_{2.5}$ concentration variation was highly correlated with meteorological conditions. We found that the higher seasonal $PM_{2.5}$ mass concentration usually occurred with higher temperature, windless and less rainfall weather, such as during spring and summer. The higher concentrations of SO_4^{2-}, NH_4^+ and OC also observed in spring and summer may result from higher temperatures and more intense solar radiation, which provide favorable conditions for photochemical activity and secondary OC production. Annual average data showed that the major chemical components of $PM_{2.5}$ were SO_4^{2-}, NO_3^-, NH_4^+, OCM, EC and crustal elements. Comparing with the data at the urban sites of Kameda and Chiba, lower concentrations of EC and NO_3^- and higher OC/EC ratios were observed at the Niigata-Maki site. EC is considered as a tracer of diesel emission or fossil fuel combustion of stationary sources, and the vehicular traffic is also a significant source of gaseous precursors (NO_x) and formed secondary aerosol of nitrate. Therefore, the observational results suggested that there was no significant stationary source and low vehicular traffic around the site. The higher OC/EC ratio at the Niigata-Maki site is also representative of a rural site.

$PM_{2.5}$ source apportionment was characterized by positive matrix factorization (PMF) analysis, and the results inferred four major emission sources: sea salt, biomass combustion, soil dust and secondary aerosol. The relative contributions of the four major sources to $PM_{2.5}$ concentrations at Niigata-Maki were 10.2% for sea salt, 18.9% for biomass combustion, 13.2% for soil dust and 44.4% for secondary aerosol, respectively. We performed a potential source contribution function (PSCF) analysis to identify potential source regions of the four major sources. The high value PSCF plots suggested that the Sea of Japan was the main source area of sea salt. The major source region of biomass combustion was from northeast China in autumn, and local areas in Niigata and southwest Japan were the main source areas in other seasons. The major source area of soil dust was northeast China in winter, while the contributions of local areas in Niigata and the Sea of Japan were more remarkable in other seasons. The secondary aerosol of $(NH_4)_2SO_4$ was mainly originated from southwest Japan. The PMF analysis and correlation results showed a relationship between $(NH_4)_2SO_4$ with oil or coal combustion source. Thermal power plants are concentrated in the southwest of Japan and Tokyo metropolitan area. Coal or oil burning factories and volcanoes were also the potential source of SO_4^{2-} in Japan. The concentrations of SO_4^{2-} and NH_4^+ were obviously high in summer, when the Pacific high covers the mainland in Japan and the air mass is usually transported along the ridge of the Pacific high. Moreover, the central mountains in Japan will hinder transportation from Tokyo metropolitan area. Therefore, southwest Japan was the major source region of secondary aerosol.

Comparing with previous source apportionment studies in western Japan, this study showed the regional characteristics of $PM_{2.5}$ sources at Niigata-Maki station in eastern Japan. A large domestic contribution from southwest Japan was observed for secondary aerosol, while a larger contribution of long range transportation from the NEA was observed in previous studies. Significant contribution of biomass combustion from local or long range transportation was uniquely observed. These results and scientific findings can be used for an evaluation of the atmospheric impact of $PM_{2.5}$ at Niigata-Maki station in eastern Japan.

ACKNOWLEDGMENTS

This work was partly supported by JSPS KAKENHI Grant Number 25502005 and Environment Research and Technology Development Fund (5-1306) of the Ministry of the Environment, Japan.

SUPPLEMENTARY MATERIAL

Supplementary data associated with this article can be

found in the online version at http://www.aaqr.org.

REFERENCES

Aikawa, M., Ohara, T., Hiraki, T., Oishi, O., Tsuji, A., Yamagami, M., Murano, K. and Mukai, H. (2010). Significant geographic gradients in particulate sulfate over Japan determined from multiple-site measurements and a chemical transport model: Impacts of transboundary pollution from the Asian continent. *Atmos. Environ.* 44: 381–391.

Almeida, S.M., Lage, J., Fernandez, B., Garcia, S., Reis, M.A. and Chaves, P.C. (2015). Chemical characterization of atmospheric particles and source apportionment in the vicinity of a steelmaking industry. *Sci. Total Environ*. 521–522: 411–420.

Amato, F. and Hopke, P.K. (2012). Source apportionment of the ambient $PM_{2.5}$ across St. Louis using constrained positive matrix factorization. *Atmos. Environ*. 46: 329–337.

Bao, L., Sekiguchi,K., Wang, Q. and Sakamoto, K. (2009). Comparison of water-soluble organic components in size-segregated particles between a roadside and a suburban site in Saitama, Japan. *Atmos. Environ*. 9: 412–420.

Bell, M.L., Dominici, F., Ebisu, K., Zeger, S.L. and Samet, J.M. (2007). Spatial and temporal variation in $PM_{2.5}$ chemical composition in the United States for health effects studies. *Environ. Health Perspect*. 115: 989–995.

Brown, S.G., Eberly, S., Paatero, P. and Norris, G.A. (2015). Methods for estimating uncertainty in PMF solutions: Examples with ambient air and water quality data and guidance on reporting PMF results. *Sci. Total Environ.* 518–519: 626–635.

Chan, C.C., Chuang, K.J., Chien, L.C., Chen, W.J. and Chang, W.T. (2006). Urban air pollution and emergency admissions for cerebrovascular diseases in Taipei, Taiwan. *Eur. Heart J.* 27: 1238–1244.

Chen, Y., Schleicher, N., Chen, Y., Chai, F. and Norra, S. (2014). The influence of governmental mitigation measures on contamination characteristics of $PM_{2.5}$ in Beijing. *Sci. Total Environ.* 490: 647–658.

Chow, J.C., Watson, J.G., Crow, D., Lowenthal, H.D. and Merrifield, T. (2001). Comparison of IMPROVE and NIOSH carbon measurements. *Aerosol Sci. Technol.* 34: 23–34.

Coulibaly, S., Minami, H., Abe, M., Hasei, T., Oro, T., Funasaka, K., Daichi, A., Masanari, W., Naoko, H., Keiji, W. and Watanabe, T. (2015). Long-range transport of mutagens and other air pollutants from mainland East Asia to western Japan. *Genes Environ.* 37: 1–10.

Csavina, J., Field, J., Felix, O., Alba, Y., Avitia, C., Saez, A.E. and Betterton, E.A. (2014). Effect of wind speed and relative humidity on atmospheric dust concentrations in semi-arid climates. *Sci. Total Environ*. 487: 82–90.

de Gouw, J.A. and Jimenez, J.L. (2009). Organic aerosols in the earth's atmosphere. *Environ. Sci. Technol*. 43: 7614–7618.

Electrical Japan, http://agora.ex.nii.ac.jp/earthquake/201103-eastjapan/energy/ electrical-japan/ type/1.html.ja. Last Access: 21 April 2017.

Fabretti, J.F., Sauret, N., Gal, J.F., Maria, P.C. and Schärer, U. (2009). Elemental characterization and source identification of $PM_{2.5}$ using Positive Matrix Factorization: The Malraux road tunnel, Nice, France *Atmos. Res*. 94: 320–329.

Furuta, N., Iijima, A., Kambe, A., Sakai, K. and Sato, K. (2005). Concentrations, enrichment and predominant sources of Sb and other trace elements in size classified airborne particulate matter collected in Tokyo from 1995 to 2004. *J. Environ. Monit.* 7: 1155–1161.

Gao, Y., Nelson, D.E., Field, P.M., Ding, Q., Li, H., Sherrell, R.M., Gigliotti, C.L., Ryda, V., Glenn, T.R. and Eisenreich, S.J. (2002). Characterization of atmospheric trace elements on $PM_{2.5}$ particulate matter over the New York–New Jersey harbor estuary. *Atmos. Environ.* 36: 1077–1086.

Hering, S. and Cass, G. (1999). The magnitude of bias in measurement of $PM_{2.5}$ arising from volatilization of particulate nitrate from Teflon filters. *J. Air Waste Manage. Assoc.* 49: 725–733.

Hueglin, C., Gehrig, R., Baltensperger, U., Gysel, M., Monn, C. and Vonmont, H. (2005). Chemical characterisation of $PM_{2.5}$, PM_{10} and coarse particles at urban, near-city and rural sites in Switzerland. *Atmos. Environ.* 39: 637–651.

Huo, M.Q., Sato, K., Ohizumi, T., Akimoto, H. and Takahashi, K. (2016). Characteristics of carbonaceous components in precipitation and atmospheric particle at Japanese sites. *Atmos. Environ.* 146: 164–173.

Husain, L. and Dutkiewicz, V.A. (1990). A long term (1975–1988) study of atmospheric SO_4^{2-}: Regional contributions and concentration trends. *Atmos. Environ.* 24: 1175–1187.

Ichikawa, Y., Neito, S., Ishii, K. and Oohashi, H. (2015). Seasonal variation of $PM_{2.5}$ components observed in an industrial area of Chiba Prefecture, Japan. *Asian J. Atmos. Environ.* 9: 66–77.

Iijima, A., Sato, K., Yano, K., Kato, M., Kozawa, K., Furuta, N. (2008). Emission factor for antimony in brake abrasion dusts as one of major atmospheric antimony sources. *Environ. Sci. Technol.* 42: 2937–2942.

Iijima, A., Sato, K., Fujitani, Y., Fujimori, E., Saito, Y., Tanabe, K., Ohara, T., Kozawa, K. and Furuta, N. (2009). Clarification of the predominant emission sources of antimony in airborne particulate matter and estimation of their effects on the atmosphere in Japan. *Environ. Chem*. 6: 122–132.

Ikeda, K., Yamaji, K., Kanaya, Y., Taketani, F., Pan, X., Komazaki, Y., Kurokawa, J. and Ohara, T. (2014). Sensitivity analysis of source regions to $PM_{2.5}$ concentration at Fukue Island, Japan. *J. Air Waste Manage. Assoc.* 64: 445–452.

Ikeda, K., Yamaji, K., Kanaya, Y., Taketani, F., Pan, X., Komazaki, Y., Kurokawa, J. and Ohara, T. (2015). Source region attribution of $PM_{2.5}$ mass concentrations over Japan. *Geochem. J.* 49: 185–194.

Inomata, Y., Ohizumi, T., Take, N., Sato, K. and Nishikawa, M. (2016). Transboundary transport of anthropogenic sulfur in $PM_{2.5}$ at a coastal site in the Sea of Japan as studied by sulfur isotopic ratio measurement. *Sci. Total Environ.* 553: 617–625.

Itahashi, S., Hayami, H., Yumimoto, K. and Uno, I. (2005).

Chinese province-scale source apportionments for sulfate aerosol in 2005 evaluated by the tagged tracer method. *Environ. Pollut.* 220: 1366–1375.

JMA (2017). http://www.jma.go.jp/jma/index.html, Last Access: 10 April 2017.

Kajino, M., Ueda, H., Sato, K. and Sakurai, T. (2011). Spatial distribution of the source-receptor relationship of sulfur in Northeast Asia. *Atmos. Chem. Phys*. 11: 6475–6491.

Kaneyasu, N., Yamamoto, S., Sato, K., Takami, A., Hayashi, M., Hara, K., Kawamoto, K., Okuda, T. and Hatakeyama, S. (2014). Impact of long-range transport of aerosols on the $PM_{2.5}$ composition at a major metropolitan area in the northern Kyushu area of Japan. *Atmos. Environ.* 97: 416–425.

Kennish, M.J. (1994). *Practical handbook of marine science*, CRC Press, Boca Raton.

Khan, M. F., Shirasuna, Y., Hirano, K. and Masunaga, S. (2010). Characterization of $PM_{2.5}$, $PM_{2.5–10}$ and $PM_{>10}$ in ambient air, Yokohama, Japan. *Atmos. Res.* 96: 159–172.

Kikuchi, R., Sasaki, Y., Oba, A., Sato, A., Takada, M., Fujiwara, K., Kimoto, T., Ozeki, T., Sera, K. and Ogawa, N. (2010). Origin and transportation course of heavy metal elements in the particulate matter (PM) at the Hachimantai mountain range in Northern Japan. *Soc. Mater. Eng. Resour. Japan* 17: 177–181.

Kim, E., Hopke, P.K. and Edgerton, E.S. (2004). Improving source identification of Atlanta aerosol using temperature resolved carbon fractions in positive matrix factorization. *Atmos. Environ*. 38: 3349–3362.

Kumagai, K., Iijima, A., Shimoda, M., Saitoh, Y., Kozawa, K., Hagino, H. and Sakamoto, K. (2010). Determination of dicarboxylic acids and levoglucosan in fine particles in the Kanto Plain, Japan, for source apportionment of organic aerosols. *Aerosol Air Qual. Res.* 10: 282–291.

Leiva, G.M.A., Santibañez, D.A., Ibarra, E.S. and Matus, C.P. (2013). A five-year study of particulate matter ($PM_{2.5}$) and cerebrovascular diseases. *Environ. Pollu.*181: 1–6.

Liu, B., Wu, J., Zhang, J., Wang, L., Yang, J., Liang, D., Dai, Q., Bi, X., Feng, Y.C., Zhang, Y.F. and Zhang, Q.X. (2017). Characterization and source apportionment of $PM_{2.5}$ based on error estimation from EPA PMF 5.0 model at a medium city in China. *Environ. Pollut.* 222: 10–22.

Mason, B. (1966). *Principles of geochemistry*, Wiley, New York.

MOEJ (2016). http://www.env.go.jp/air/osen/pm/html, Last Access: 6 January 2016.

Murakami, Y. and Ono, M. (2006). Myocardial infarction deaths after high level exposure to particulate matter. *J. Epidemiol. Community Health* 60: 262–266.

Nakatsubo, R., Tsunetomo, D., Horie, Y., Hiraki, T., Saitoh, K., Yoda, Y. and Shima, M. (2014). Estimate of regional and broad-based sources for $PM_{2.5}$ collected in an industrial area of Japan. *Asian J. Atmos. Environ.* 8–3: 126–139.

National Institute for Environmental Studies (2015). http://www.nies.go.jp/labo/crm-e/index.html, Last Access: 12 October 2015.

Network Center for EANET (2010). *Technical manual for wet deposition monitoring in East Asia - 2010*, Asia Center for Air Pollution Research, Niigata.

Network Center for EANET (2016). *Report of the inter-laboratory comparison project 2015*, Asia Center for Air Pollution Research, Niigata.

Okuda, T., Tenmoku, M., Kato, J., Mori, J., Sato, T., Yokouchi, R. and Tanaka, S. (2006). Long-term observation of trace metal concentration in aerosols at a remote island, Rishiri, Japan by using inductively coupled plasma mass spectrometry equipped with laser ablation. *Water Air Soil Pollut*. 174: 3–17.

Ouyang, W., Guo, B.B., Cai, G.Q., Li, Q., Han, S., Liu, B. and Liu, X.G. (2015). The washing effect of precipitation on particulate matter and the pollution dynamics of rainwater in downtown Beijing. *Sci. Total Environ.* 505: 306–314.

Paatero, P. (2007). *User's guide for positive matrix factorization programs PMF2 and PMF3, Part 1-2: Tutorial, 19-21,* University of Helsinki, Helsinki, Finland.

Pang, Y., Eatough, N.L. and Eatough, D.J. (2002). $PM_{2.5}$ semivolatile organic material at riverside, California: implications for the $PM_{2.5}$ Federal Reference Method sampler. *Aerosol Sci. Technol.* 36: 277–278.

PMF 5.0 User Guide (2016). https://www.epa.gov/air-research/epa-positive-matrix-factorization-50-fundamentals-and-user-guide, Last Access: 12 May 2016.

Reimann, C. and Caritat, P. (1998). *Chemical elements in the environment: Factsheets for the geochemist and environmental scientist,* Springer, Berlin, Heidelberg.

Sanchez-Romero, A., Sanchez-Lorenzo, A., Calbo, J., Gonzalez, J.A. and Azorin-Molina, C. (2014). The signal of aerosol induced changes in sunshine duration records: A review of the evidence. *J. Geophys. Res.* 119: 4657–4673.

Shimada, K., Shimada, M., Takami, A., Hasegawa, S., Fushimi, A., Arakaki, T., Izumi, W. and Hatakeyama, S. (2015). Mode and place of origin of carbonaceous aerosols transported from East Asia to Cape Hedo, Okinawa, Japan. *Aerosol Air Qual. Res.* 15: 799–813.

Shimadera, H., Kondo, A., Kaga, A., Shrestha, K.L. and Inoue, Y. (2009). Contribution of transboundary air pollution to ionic concentrations in fog in the Kinki Region of Japan. *Atmos. Environ.* 43: 5894–5907.

Smichowski, P., Gómez, D.R., Frazzoli, C. and Caroli, S. (2008). Traffic-related elements in airborne particulate matter. *Appl. Spectrosc. Rev.* 43: 23–49.

Speight, J.G. (2014). *The chemistry and technology of petroleum*. CRC press, Boca Raton.

Tang, N., Hattori, T., Taga, R., Igarashi, K., Yang, X.Y., Tamura, K., Kakimoto, H., Mishukov, V.F., Toriba, A., Kizu, R. and Hayakawa, K. (2015). Polycyclic aromatic hydrocarbons and nitropolycyclic aromatic hydrocarbons in urban air particulates and their relationship to emission sources in the Pan–Japan Sea countries. *Atmos. Environ.* 39: 5817–5826.

Wahlin, P., Berkowicz, R. and Palmgren, F. (2006). Characterisation of traffic-generated particulate matter in Copenhagen. *Atmos. Environ.* 40: 2151–2159.

Wang, Y.Q., Zhang, X.Y. and Draxler, R. (2009). TrajStat: GIS-based software that uses various trajectory statistical analysis methods to identify potential sources from long-term air pollution measurement data. *Environ. Modell. Software* 24: 938–939.

Yamazaki, S., Nitta, H., Ono, M., Green, J. and Fukuhara, S. (2007). Intracerebral haemorrhage associated with hourly concentration of ambient particulate matter: Case-crossover analysis. *Occup. Environ. Med.* 64: 17–24.

Yang, L.X., Wang, D.C., Cheng, S.H., Wang, Z., Zhou, Y., Zhou, X.H. and Wang, W.X. (2007). Influence of meteorological conditions and particulate matter on visual range impairment in Jinan, China. *Sci. Total Environ.* 383: 164–173.

Yao, L., Yang, L.X., Yuan, Q., Yan, C., Dong, C., Meng, C.P., Sui, X., Yang, F., Lu, Y.L. And Wang, W.X. (2016). Sources apportionment of $PM_{2.5}$ in a background site in the North China Plain. *Sci. Total Environ.* 541: 590–598.

Ye, B., Ji, X., Yang, H., Yao, X., Chan, C.K., Cadle, S.H., Chan, T. and Mulawa, P.A. (2003). Concentration and chemical composition of $PM_{2.5}$ in Shanghai for a 1-year period. *Atmos. Environ.* 37: 499–510.

Zang, H.S. (2015). Long-term variations in $PM_{2.5}$ emission from open biomass burning in northeast Asia derived from satellite-derived data for 2000-2013. *Atmos. Environ.* 107: 342–350.

Zeller, M., Giroud, M., Royer, C., Benatru, I., Besancenot, J.P., Rochette, L. and Cottin, Y. (2006). Air pollution and cardiovascular and cerebrovascular disease epidemiologic data. *Presse Med.* 35: 1517–1522.

Zhang, C., Ni, Z.W. and Ni, L.P. (2015). Multifractal detrended cross-correlation analysis between $PM_{2.5}$ and meteorological factors. *Physica A* 438: 114–123.

Received for review, May 25, 2017
Revised, November 13, 2017
Accepted, November 16, 2017